4.2.2 Characteristic Features of Rainfall

The rainfall observed by MAF in and around the project area are shown in Table 4-2-3. The locations of the rain-gauges are shown in Fig. 3-1-3. The standard deviations of rainfall data are so high compared with the mean values that it suggests widely fluctuating rainfalls.

There are two periods of annual rainfall: summer and winter rainfall. Summer and winter rainfall is assumed to be during June to September and October to May, respectively.

Relations between elevation and seasonal annual rainfalls are shown in Fig. 4-2-4. This figure shows that the rainfall amounts increase by the altitude. Annual rainfall distribution estimated from this figure is shown in Fig. 4-2-5.

Muscat is the only station which can supply rainfall data for a long period (73 years intermittently from 1872) in and around the project area. The data was plotted and shown in Fig. 4-2-6. The year observed is indicated in the figure. In case no data was available for Muscat, the data observed at Dar Sait or Ruwi (MAF) near Muscat was plotted.

The total rainfall at Ruwi in two years (June, 1983 - July, 1985) was only 22 mm observed by the survey team. The two years were extremely dry.

Daily rainfall recorded at the rain-gauges installed by the Project are shown in Fig. 4-2-7. The rain-gauges (from RA3 to RK6) shown in the upper part on this figure are located in the mountain area. The rain-gauges (from RA2 to RM4) are on and around the boundary between the moutain and the marginal wadi plane area and the other (from RA1 to RM2) are in the marginal wadi plain and the gravel plain area.

The rainfall in summer were limited to the mountain and the marginal wadi plain except only one event of rainfall.

The maximum rainfall intensities are shown in Table 4-2-4. The figure shows that summer rain was only in the mountain, and winter rain was in the gravel plain. Heavy rainfall in the mountains were caused by the tropical cyclone on August 10 to 11, 1984. On the other hand the intense rainfall of short period in the mountains were recorded on various dates.

The present analysis identified three causes for the rainfalls. They are: 1) synoptic disturbances, 2) sea breeze circulation and 3) tropical cyclones. Sea breeze circulation has never been pointed out so far as the cause of the rainfall in the Batinah Coast. The rainfall characteristics of each cause are discussed below.

1) Rainfall caused by synoptic scale disturbance

A rainfall distribution on December 28, 1984 to January 1, 1985 is shown in Fig. 4-2-8 as an example of the rainfall caused by synoptic scale disturbance.

These rainfalls occur mainly in winter. The front, extending from the cyclone and moving easterly, brought rain over wide area, both in the mountain and in the gravel plain.

2) Rainfall caused by sea breeze

A rainfall distribution on August 25, 1984 is shown in Fig. 4-2-9. It is an example of the rainfall caused by sea breeze circulation.

These rainfalls occur mainly in summer. The mechanism of rain formation is illustrated in Fig. 4-2-10.

The sea breeze transports humid air from the Gulf of Oman to the Hajar Mountain. Then the humid air mass rises and changes to cumulus or cumulonimbus clouds, which cause an intense and short rainfall over a narrow area in the mountain.

3) Rainfall caused by tropical cyclones

The rainfall distribution on August 10 to 11, 1983 is shown in Fig. 4-2-11 as an example of the rainfall caused by a tropical cyclone.

Tropical cyclones, developed at the Indian Ocean or the Arabian Sea and move westerly with heavy rainfall. It is reported that in a few occasions tropical cyclones attack the Batinah Coast. The tropical cyclone with rainfall of more than 10 mm at Muscat comes once in more than 50 years (Renardet Sauti ICE).

Table 4-2-3 Summary of Rainfall Data Observed by MAF (1974-1984)

(unit: mm)

Site	Elevation (m)	Jan.	Feb.	Mar.	Apr.	May	June	July	Aug.	Sep.	Oct.	Nov.	Dec.	Annual
Saham	5	7.3 (11.5)	22.2 (27.8)	22.2 (38.9)	1.3 (3.6)	4.3 (14.4)	0.0 (-)	0.0 (-)	0.1 (0.2)	0.1 (0.3)	2.7 (8.9)	0.9 (2.9)	14.6 (30.2)	69.7 (51.2)
Sohar	20	9.3 (20.5)	44.7 (48.3)	14.7 (22.3)	13.3 (19.3)	1.8 (4.1)	0.0 (-)	0.3 (1.1)	0.6 (1.9)	0.4 (1.5)	4.3 (11.0)	3.2 (6.8)	8.8 (17.5)	101.4 (82.6)
Al-Ghozaifah	480	5.9 (9.5)	32.9 (36.2)	14.6 (26.8)	13.5 (24.9)	5.7 (8.1)	2.4 (7.5)	1.8 (3.2)	11.6 (16.0)	4.8 (12.1)	5.4 (8.6)	2.0 (5.6)	2.9 (6.3)	103.5 (73.5)
Al-Qufais	600	9.1 (12.7)	33.5 (40.5)	28.6 (59.9)	11.9 (25.0)	5.2 (9.1)	5.9 (10.4)	6.4 (10.5)	10.5 (16.0)	8.7 (16.0)	1.8 (5.0)	1.0 (3.2)	2.9 (8.8)	121.2 (102.8)
Haibi	570	8.3 (16.6)	44.2 (51.0)	19.3 (30.0)	10.5 (19.6)	6.7 (9.3)	6.7 (13.7)	10.1 (14.3)	11.2 (22.5)	9.1 (12.3)	13.9 (18.1)	2.2 (4.8)	0.9 (2.6)	134.9 (88.7)
Al-Houqain	225	12.2 (18.8)	30.0 (41.8)	12.6 (18.3)	14.6 (28.2)	7.5 (19.4)	0.9 (3.0)	2.9 (6.5)	2.1 (4.0)	1.4 (4.5)	16.7 (29.3)	13.9 (30.8)	19.9 (26.1)	132.4 (101.7)
Al-Rustaq	350	11.5 (15.4)	25.9 (35.5)	25.0 (37.9)	16.8 (18.9)	5.7 (10.3)	4.8 (14.2)	6.5 (11.9)	13.4 (25.7)	4.4 (5.9)	31.3 (30.3)	10.9 (16.2)	7.9 (13.9)	158.5 (105.2)
Afi	170	13.1 (14.2)	41.8 (50.7)	19.1 (24.5)	10.8 (16.5)	3.3 (9.9)	3.8 (10.3)	3.3 (6.7)	1.8 (3.4)	1.9 (4.4)	7.6 (16.8)	5.2 (13.0)	8.4 (12.3)	118.7 (88.0)
Al-Rumais	15	4.4 (9.4)	27.7 (31.0)	11.0 (20.5)	9.7 (16.6)	5.1 (16.9)	1.2 (3.6)	0.0 (-)	0.0 (-)	0.0 (-)	1.7 (4.5)	3.4 (8.0)	9.1 (17.1)	73.0 (66.0)
Saiq	2000	19.4 (23.1)	53.2 (77.6)	44.3 (49.1)	43.1 (63.8)	27.1 (31.1)	17.7 (14.4)	40.3 (43.0)	55.1 (42.2)	14.7 (11.2)	7.1 (8.9)	2.6 (3.9)	8.5 (17.1)	333.1 (146.9)

upper row: monthly mean rainfall
lower row: (standard deviation)

Table 4-2-4 Maximum Rainfall Intensities

Rain gauge		Duration							
		15 min.	30 min.	60 min.	120 min.	6 hr.	12 hr.	24 hr.	48 hr.
WADI AHIN	RA1	8.5 (29/12/84)	9.0 (29/12/84)	15.5 (29/12/84)	17.0 (29/12/84)	26.0 (29/12/84)			
	RA2	3.5 (10/8/83)	4.0 (10/8/83)	4.0 (10/8/83)	7.5 (10/8/83)	11.5 (10/8/83)	18.5 (10,11/8/83)	20.0 (10,11/8/83)	
	RA3	9.0 (29/8/83)	12.5 (29/8/83)	13.0 (29/8/83)	15.0 (10/8/83)	29.5 (10/8/83)	41.5 (10,11/8/83)	48.0 (10,11/8/83)	49.5 (10,11/8/83)
	RA4	5.0 (15/7/84)	5.0 (15/7/84)	7.5 (15/7/84)	8.0 (15/7/84)				
	RA5	10.0 (5/9/84)	19.0 (5/9/84)	20.5 (5/9/84)					
WADI BANI GHAFIR	RG1	19.5 (29/12/84)	19.5 (29/12/84)	20.5 (29/12/84)	24.0 (29/12/84)	26.0 (29/12/84)	26.0 (29/12/84)	28.0 (29/12/84)	
	RG2	12.5 (29/12/84)	12.5 (29/12/84)	16.0 (29/12/84)	16.0 (29/12/84)	18.5 (29/12/84)			
	RG3	10.0 (15/9/83)	14.0 (15/9/83)	16.0 (15/9/83)	16.5 (15/9/83)				
	RG4	13.0 (28/7/83)	13.5 (28/7/83)	13.5 (28/7/83)	13.5 (28/7/83)	28.0 (28/7/83)	37.0 (10/8/83)		
	RG5	10.0 (10/8/83)	16.5 (10/8/83)	17.5 (10/8/83)	18.0 (10/8/83)	30.0 (10/8/83)	32.5 (10/8/83)	37.0 (10/8/83)	
WADI AL-FARA'	RF1	13.5 (10/7/84)	14.5 (10/7/84)	23.0 (10/8/83)	34.5 (10/8/83)	61.5 (10/8/83)	88.5 (10/8/83)		
	RF2	19.5 (22/6/85)	26.0 (22/6/85)	26.5 (22/6/85)	39.0 (10/8/83)	53.0 (10/8/83)	54.0 (10/8/83)		
	RF3	12.5 (10/7/83)	14.0 (11/4/84)	14.0 (11/4/84)	14.0 (11/4/84)	15.0 (10/8/83)	18.5 (10/8/83)	19.5 (10,11/8/83)	
	RF4	12.0 (29/12/84)	12.5 (29/12/84)	12.5 (29/12/84)	12.5 (29/12/84)	15.5 (29/12/84)			
	MF1	3.0 (29/12/84)	5.0 (29/12/84)	7.0 (29/12/84)	9.0 (29/12/84)				
	MF2	6.4 (28/8/83)	11.0 (28/8/83)	17.6 (28/8/83)	19.0 (28/8/83)	19.0 (28/8/83)	20.4 (10/8/83)	21.0 (10/8/83)	21.2 (10,11/8/83)
WADI BANI KHARUS	RK1	15.0 (8/9/84)	20.0 (8/9/84)	20.5 (8/9/84)					
	RK2	14.0 (24/8/84)	18.0 (24/8/84)	19.0 (24/8/84)					
	RK3	18.0 (25/8/84)	35.0 (25/8/84)	43.0 (25/8/84)					
	RK4	15.0 (15/6/85)	18.0 (15/6/85)	19.5 (10/8/83)	20.0 (10/8/83)	25.0 (10/8/83)	25.5 (10/8/83)		
	RK5	16.0 (15/9/83)	18.5 (15/9/83)	19.5 (15/9/83)					
	RK6	15.5 (3/9/84)	15.5 (3/9/84)	23.0 (25/7/83)	23.0 (25/7/83)	33.5 (10/8/83)	39.5 (10/8/83)	72.0 (10,11/8/83)	
WADI AL-MA'AWIL	RM1	27.0 (29/12/84)	29.5 (29/12/84)	29.5 (29/12/84)	37.5 (29/12/84)	38.5 (29/12/84)			
	RM2	4.5 (29/12/84)	4.5 (29/12/84)	4.5 (29/12/84)	5.0 (29/12/84)	7.0 (29/12/84)			
	RM3	2.5 (10/8/83)	2.5 (10/8/83)	4.5 (10/8/83)	5.5 (10/8/83)	10.0 (10/8/83)	11.5 (10/8/83)		
	RM4	18.5 (18/4/85)	18.5 (18/4/85)	18.5 (18/4/85)	18.5 (18/4/85)	18.5 (18/4/85)	18.5 (18/4/85)	18.5 (18/4/85)	23.5 (18,19/4/85)

upper row: Rainfall (mm)
lower row: (date)

Fig. 4-2-4 Relation between Elevation and Seasonal and Annual Rainfall (1974-1984)

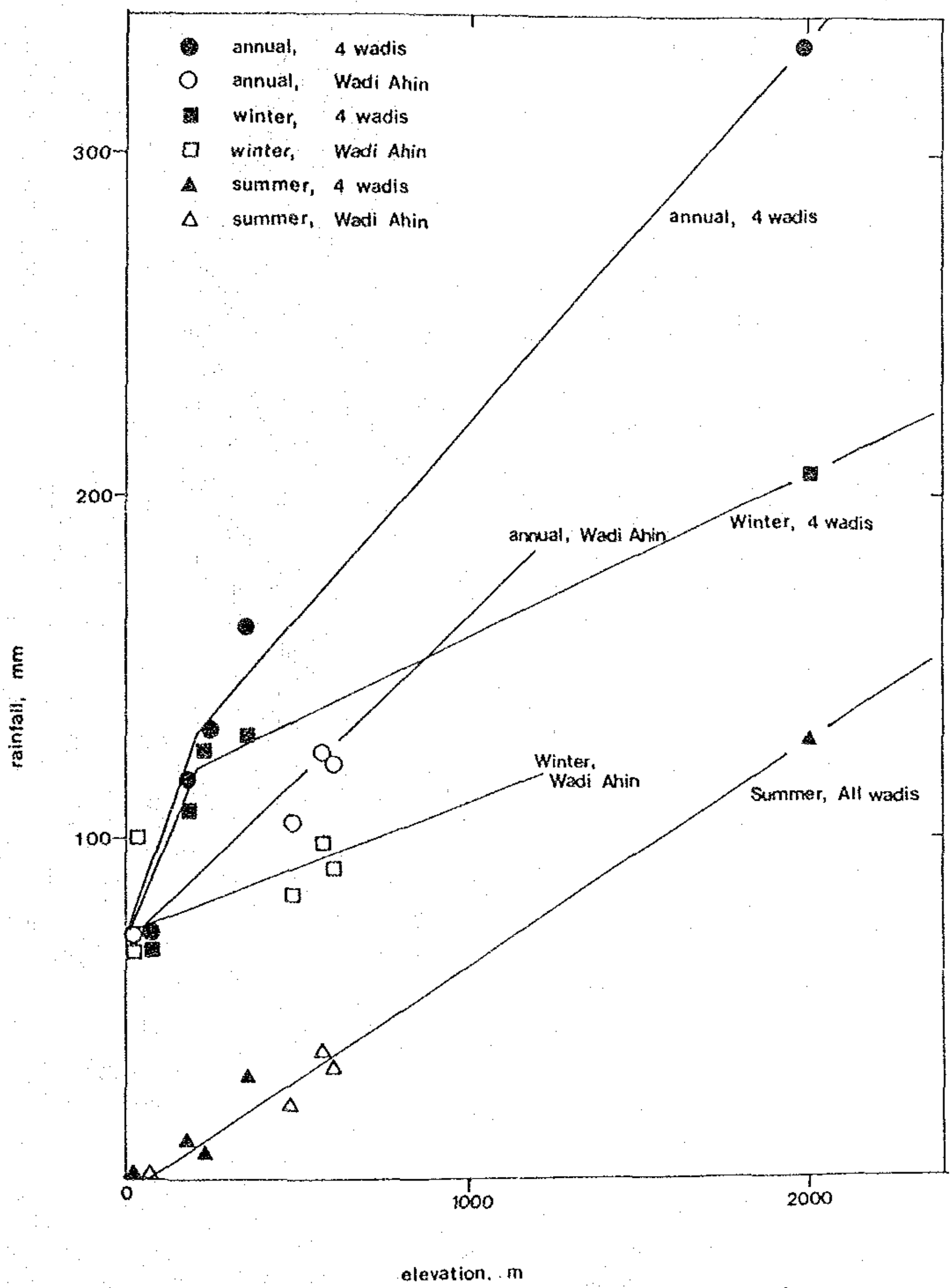

Note: 1) 4 Wadi: Wadi Bahi Ghafir, Wadi Al-Farà Wadi Bani Kharus and Wadi Al-Ma'awil

2) 2,000 m data are represented by Saiq rainfall gauge, located outside the Batinah Coast watershed, south of the mountain divide.

Fig. 4-2-5

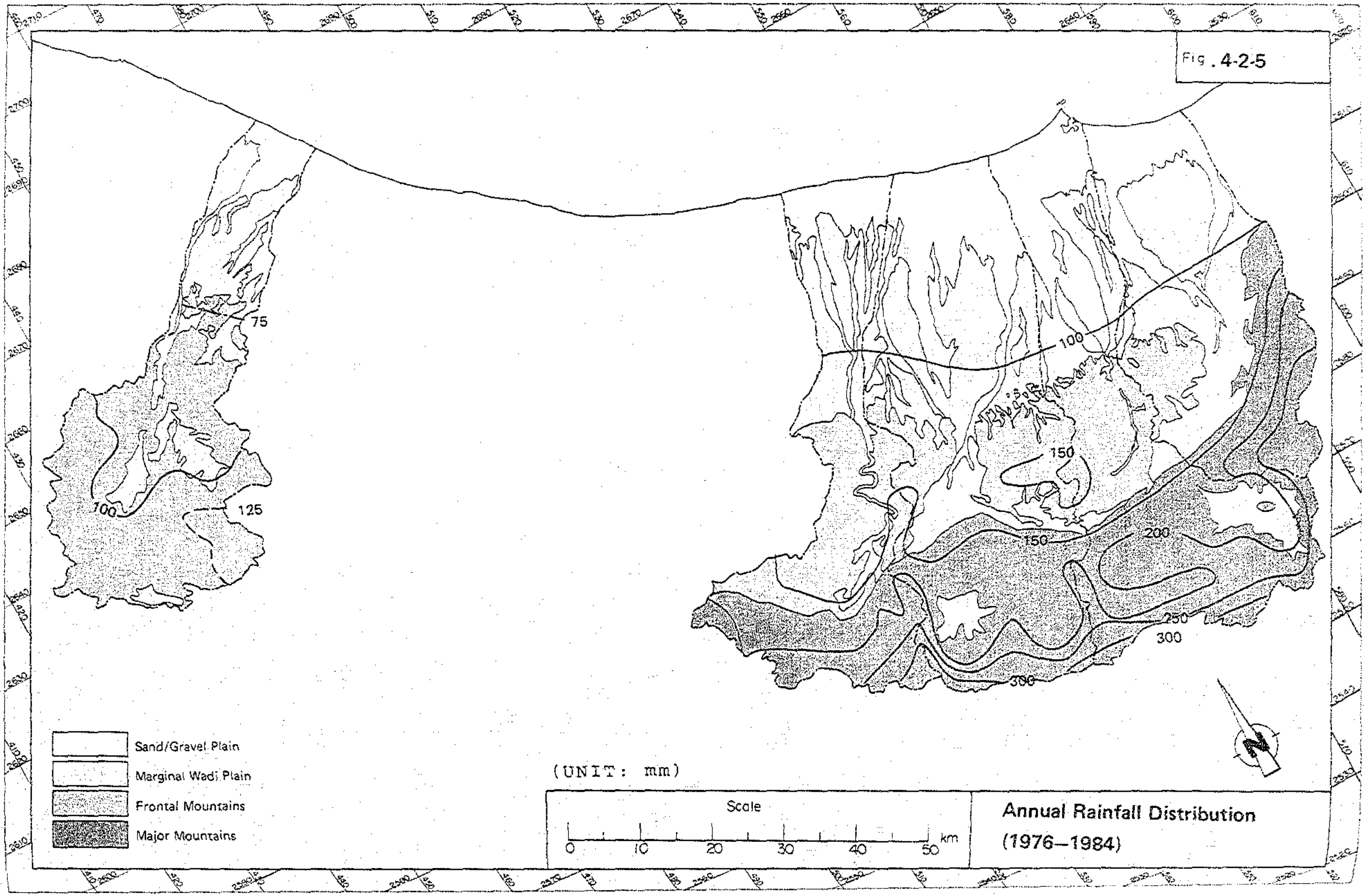

Annual Rainfall Distribution
(1976–1984)

Fig. 4-2-6 Annual Rainfall Frequency at Muscat

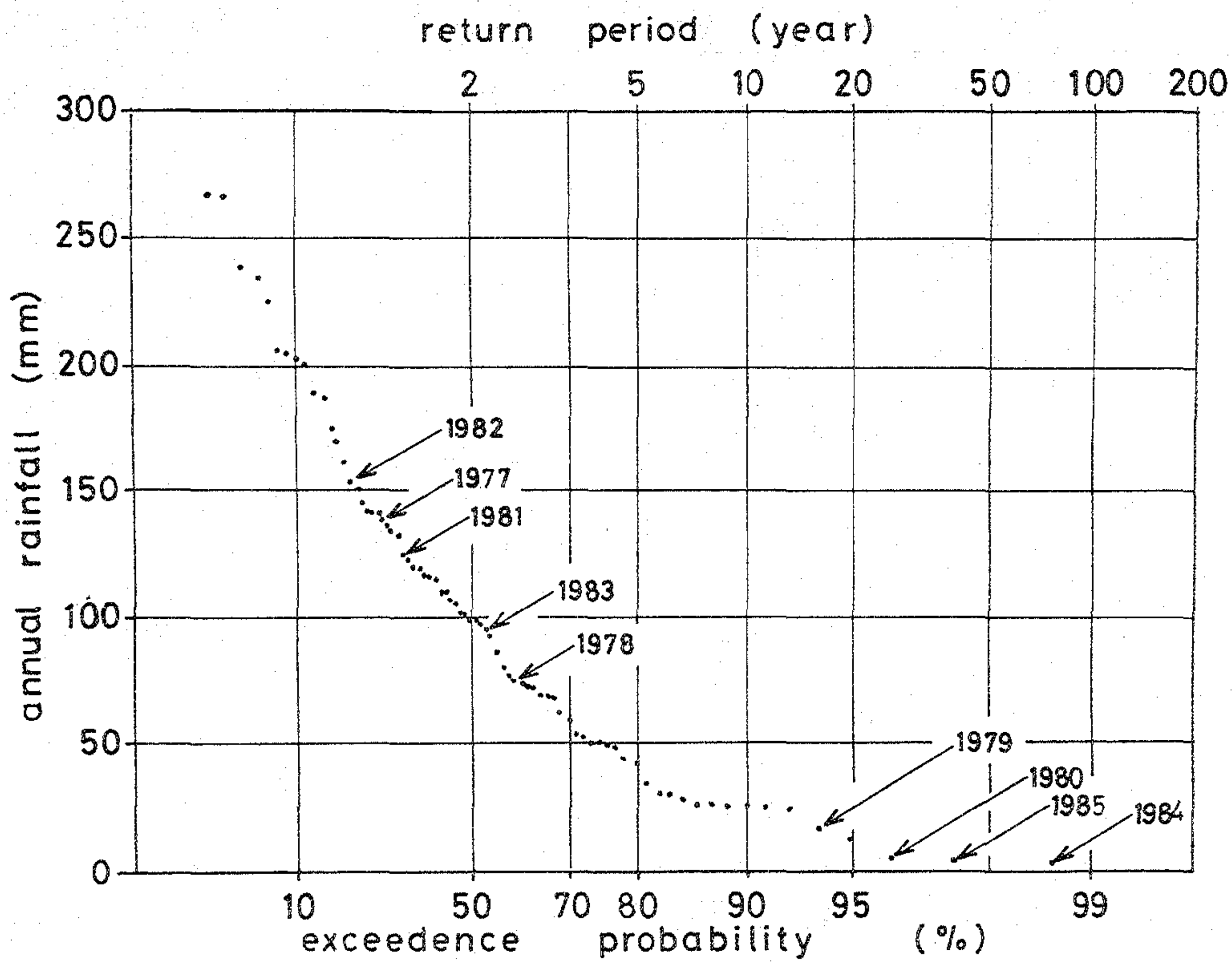

Fig. 4-2-7 Daily Rainfall Time Series

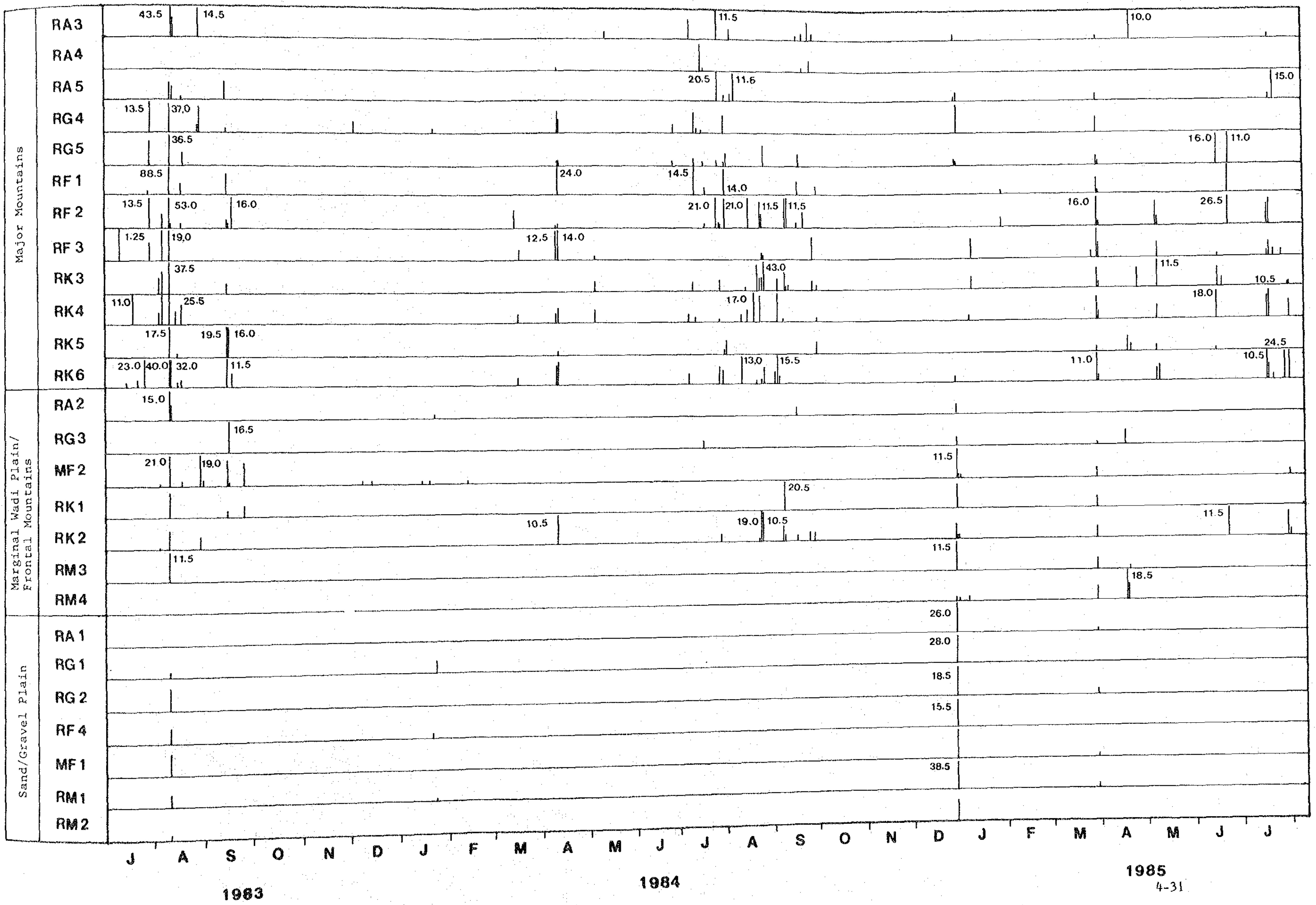

Fig . 4-2-8

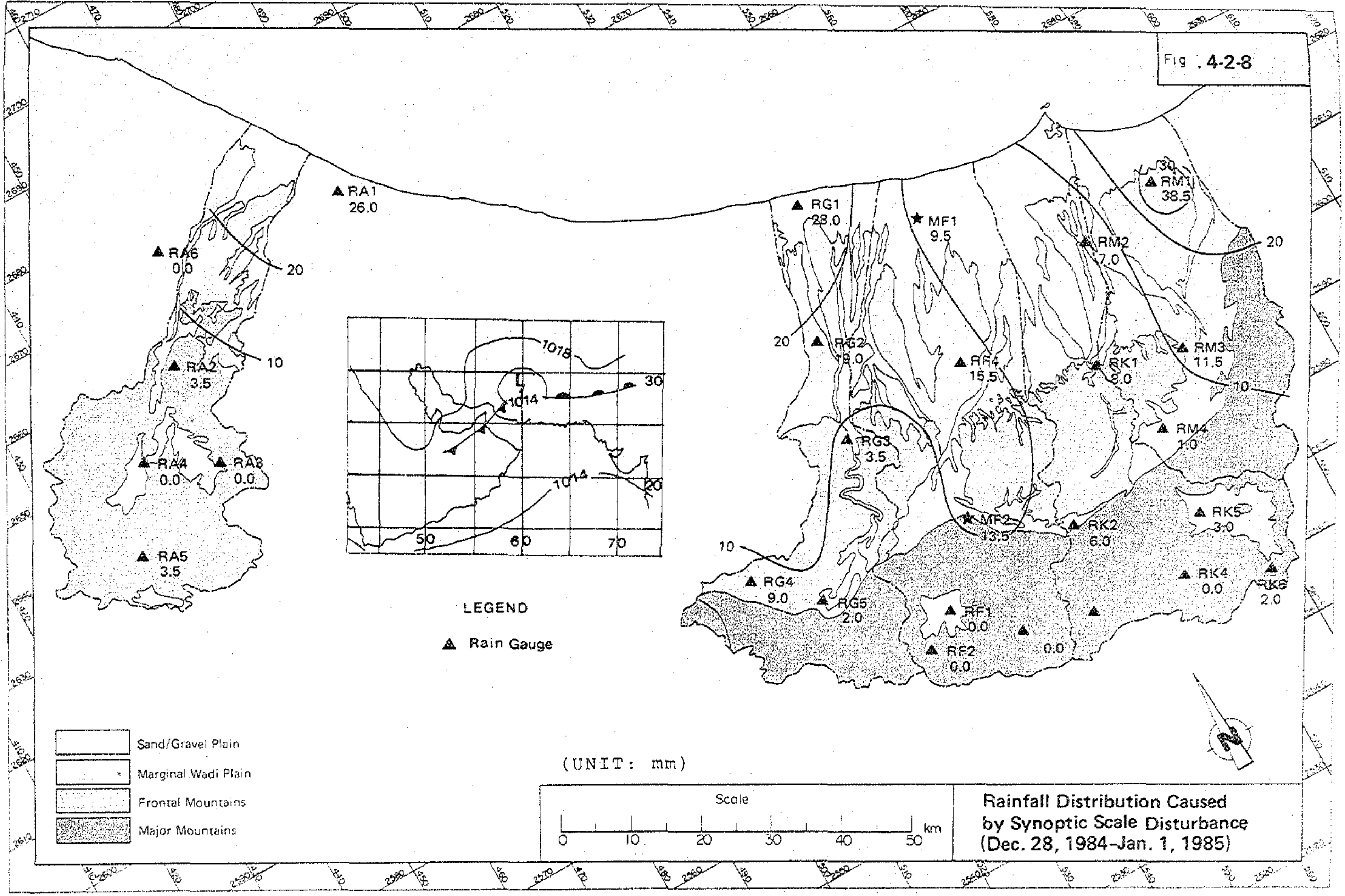

Rainfall Distribution Caused by Synoptic Scale Disturbance (Dec. 28, 1984–Jan. 1, 1985)

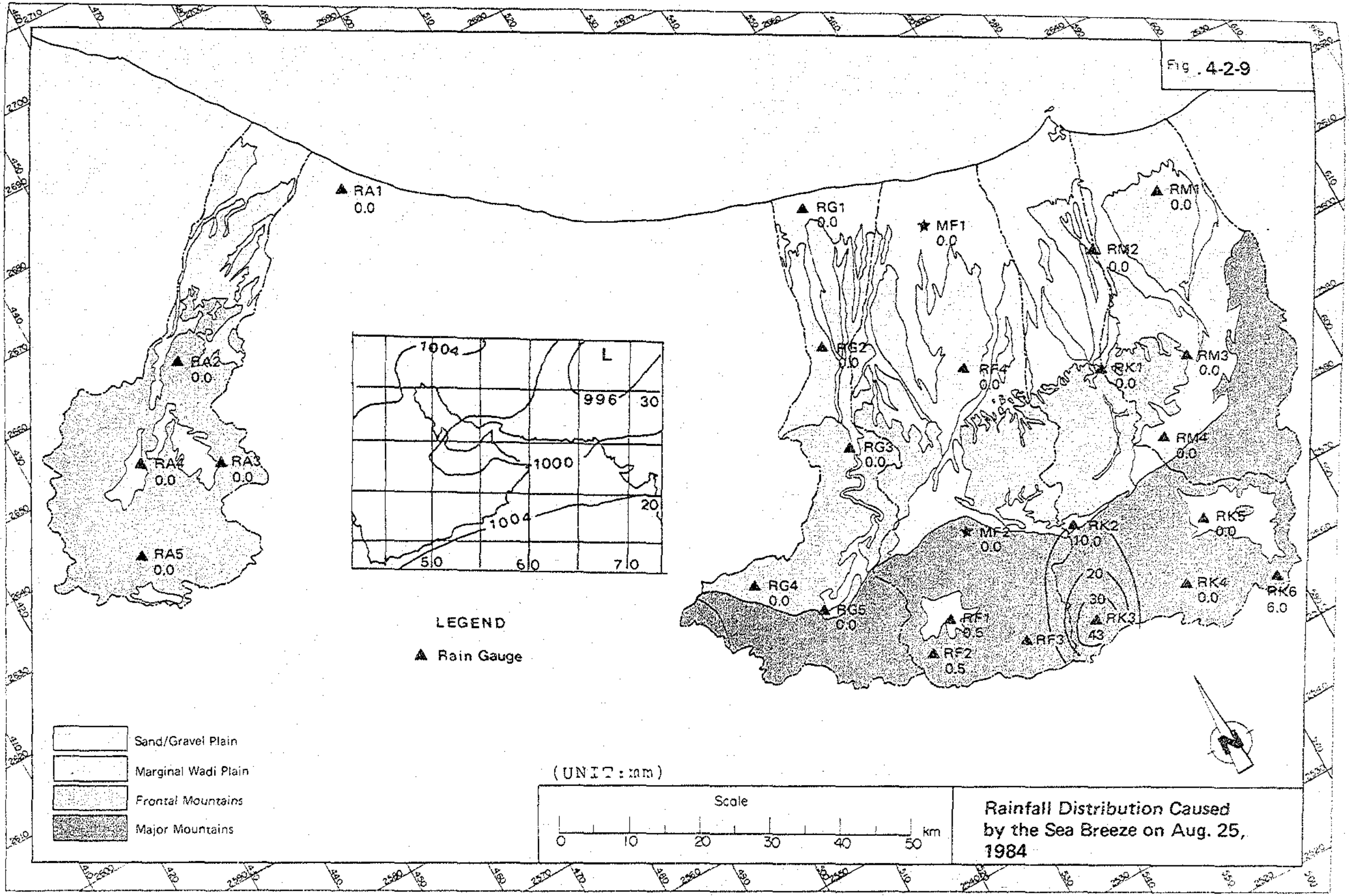

Fig. 4-2-9 Rainfall Distribution Caused by the Sea Breeze on Aug. 25, 1984

Fig. 4-2-10 Sea Breeze Circulation in the Batinah Coast

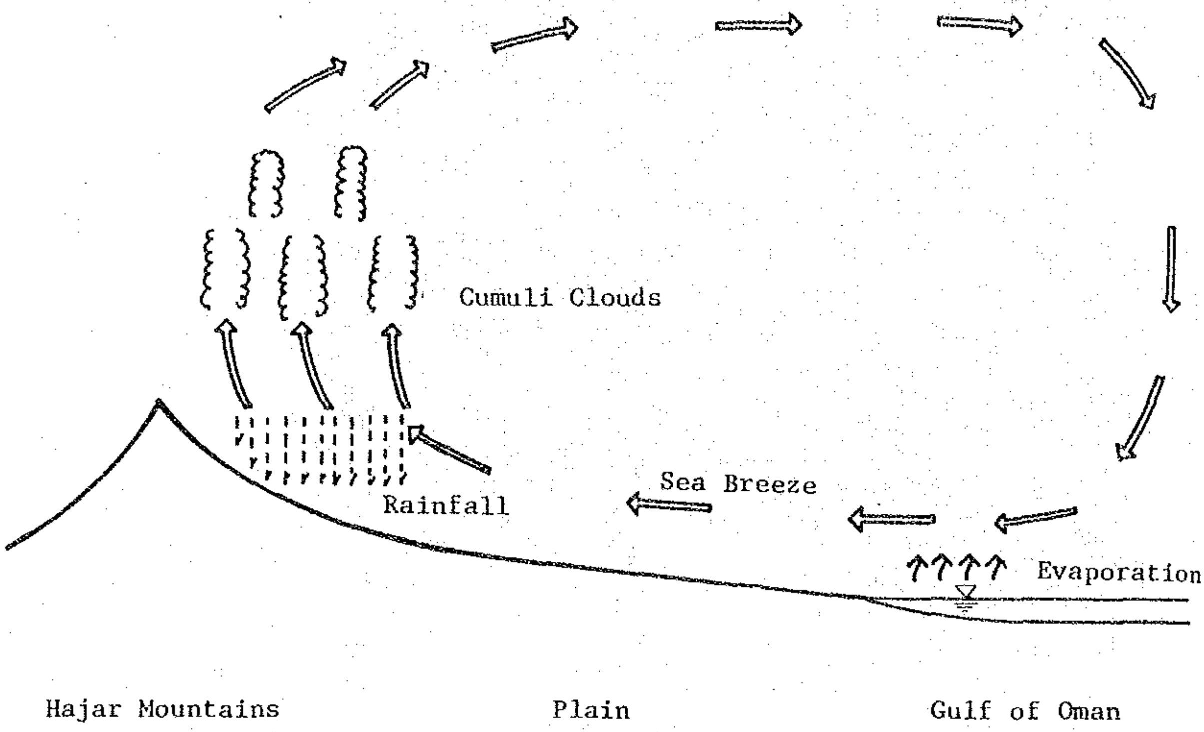

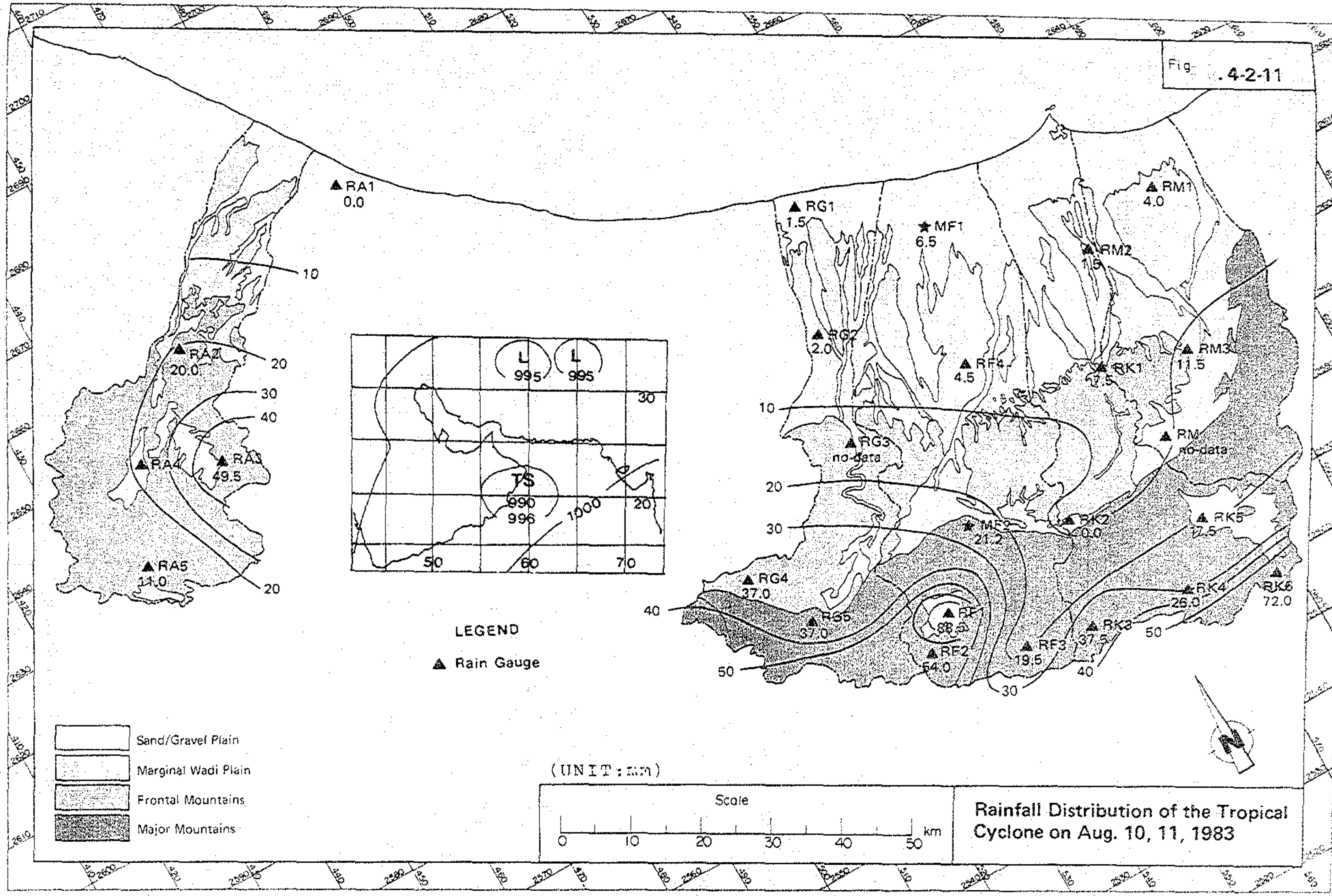

Fig. 4-2-11

Rainfall Distribution of the Tropical Cyclone on Aug. 10, 11, 1983

4.2.3 Surface Runoff

(1) Observed Surface Runoff

During the survey period, surface runoff was observed eight times at six of the wadi gauges installed by the Project. However, large floods which reach the sea did not occur in the project period as expected.* The survey period was an extremely dry. Further investigation will be required for studying the relationship between the precipitation and topographic features. The eight flood discharges recorded during the survey period are summarized in Table 4-2-5 and Fig. 4-2-13 (1), (2).

Manning's equation was used to estimate outflow from the water level data, given the geometry of wadi channel found by surveying. The roughness coefficient was assumed as 0.04 according to the wadi bed and bank materials. The ground surveys such as longitudinal profile and cross-section leveling surveys were executed at all the gauge sites during the survey period. The result of survey (WG1) is shown in Fig. 4-2-14 and other sites are attached in Supporting Report B.

Table 4-2-5 Observed Floods during Survey Period

Wadi Basin	Discharge Site	Date	Duration	Outflow (m^3)	Peak Discharge (m^3/sec)
Wadi Al-Fara'	WF1 (Mazahit)	Sep.15,'83	15:50-00:02	26,040	5.8
Wadi Bani Ghafir	WG1 (Al-Houqain)	Sep.15'83	13:46-20:57	1,263	0.9
Wadi Al-Fara'	WF4 (Tabaqah)	Apr.12,'84	14:55-16:15	815	0.7
Wadi Al-Fara'	WF1 (Mazahit)	Jul.30'84	18:00-22:01	65,017	13.0
Wadi Ahin	WA1 (Al-Heil)	Sep.15,'84	17:00-18:08	2,036	1.6
Wadi Ahin	WA1 (Al-Heil)	Sep.16'84	19:25-22:52	8,376	1.7
Wadi Al-Ma'awil	WM2 (Afi)	Apr.18,'85	16:10 - 20:07	41,891	19.1
Wadi Bani Kharus	WK1 (Al-Abiyad)	Apr.19,'85	16:20-06:51	127,658	44.1

Note: * Flood and rainfall covered the project area occured on Feb. 1, 1986. (Supporting Report H. Observed Data of Rainfall/Flood on Feb. 1, 1986).

Fig . 4-2-12

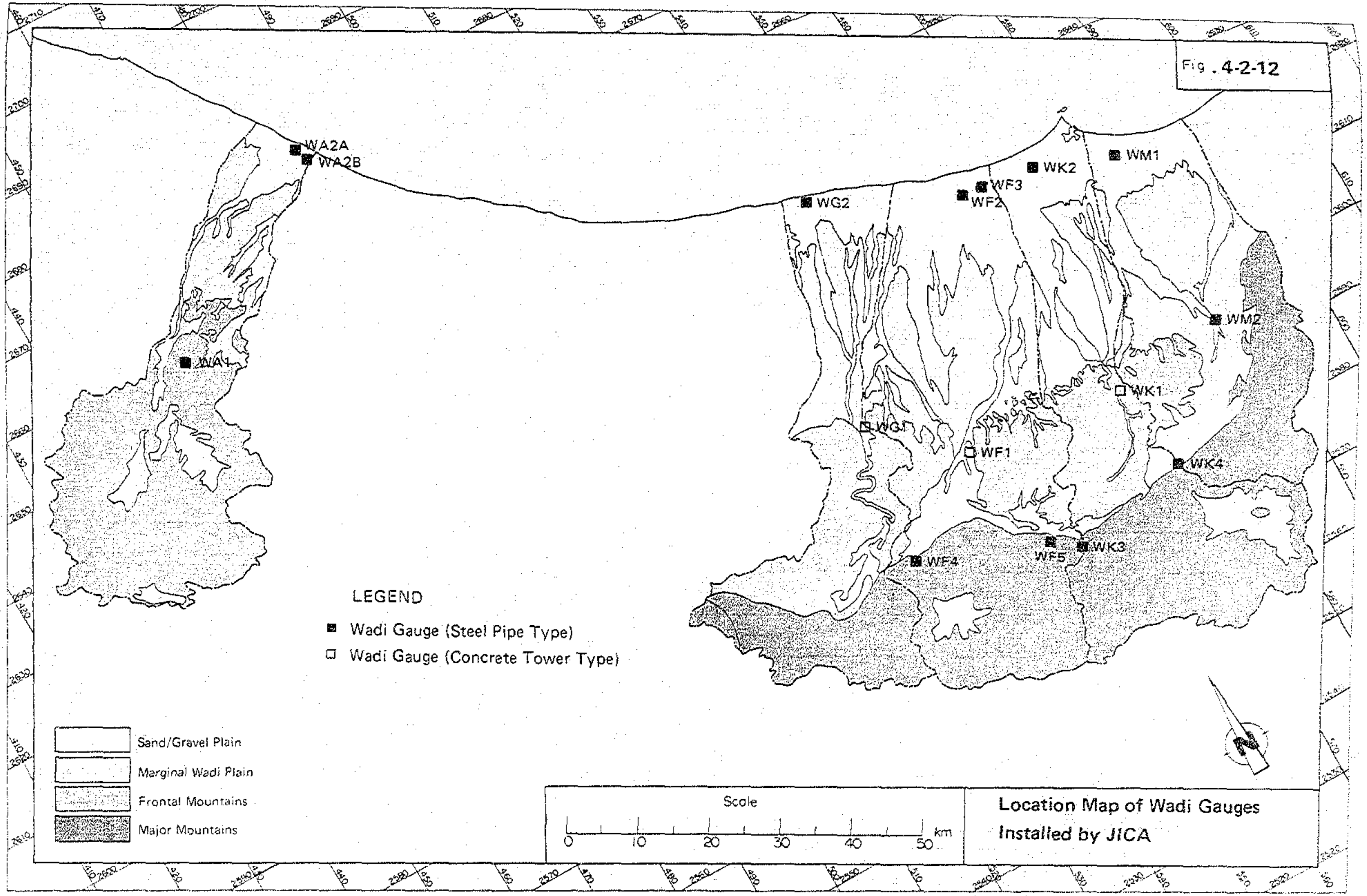

Location Map of Wadi Gauges
Installed by JICA

Fig. 4-2-13(1) Hydrographs during Survey Period (1/2)

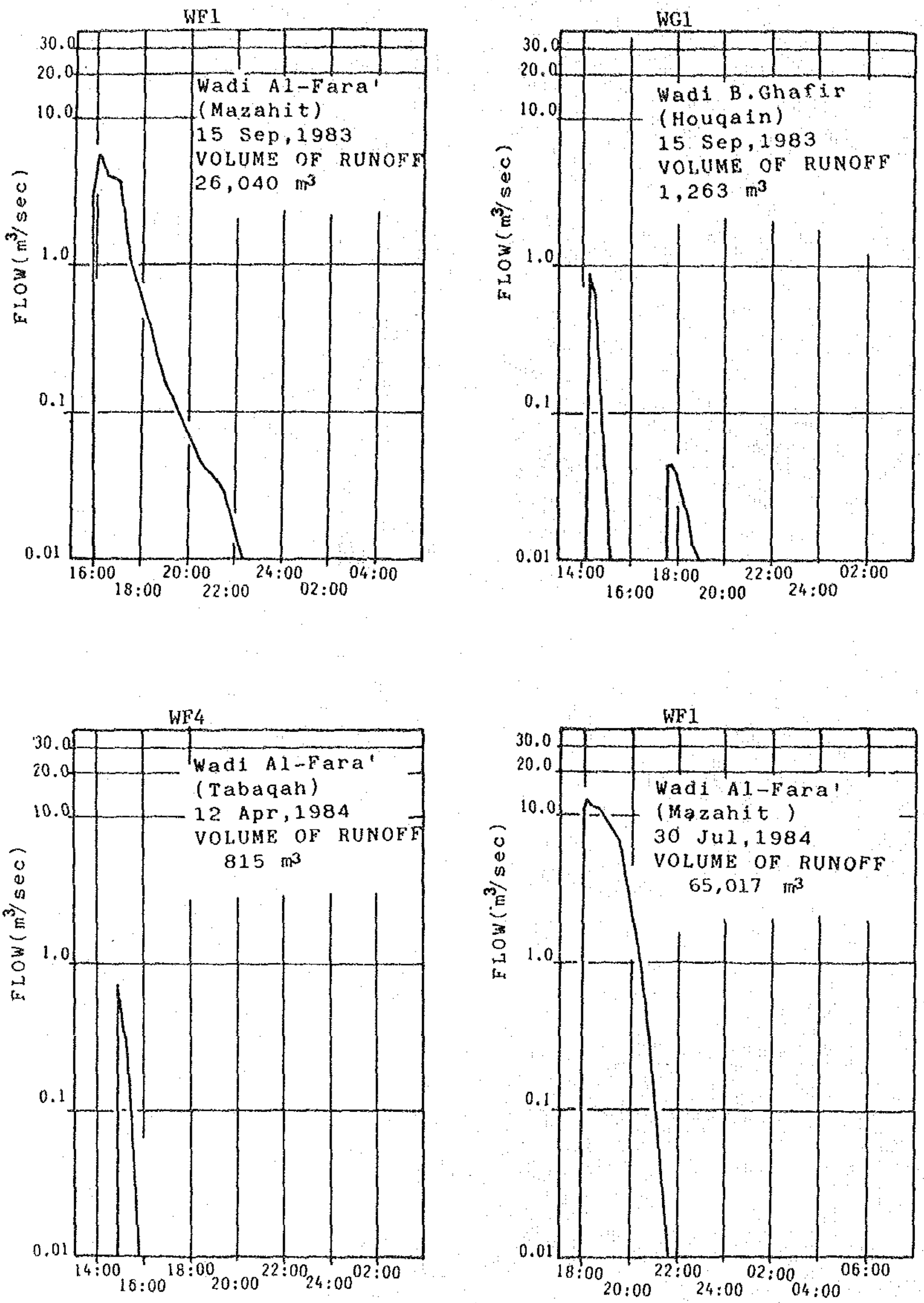

Fig. 4-2-13(2) Hydrographs during Survey Period (2/2)

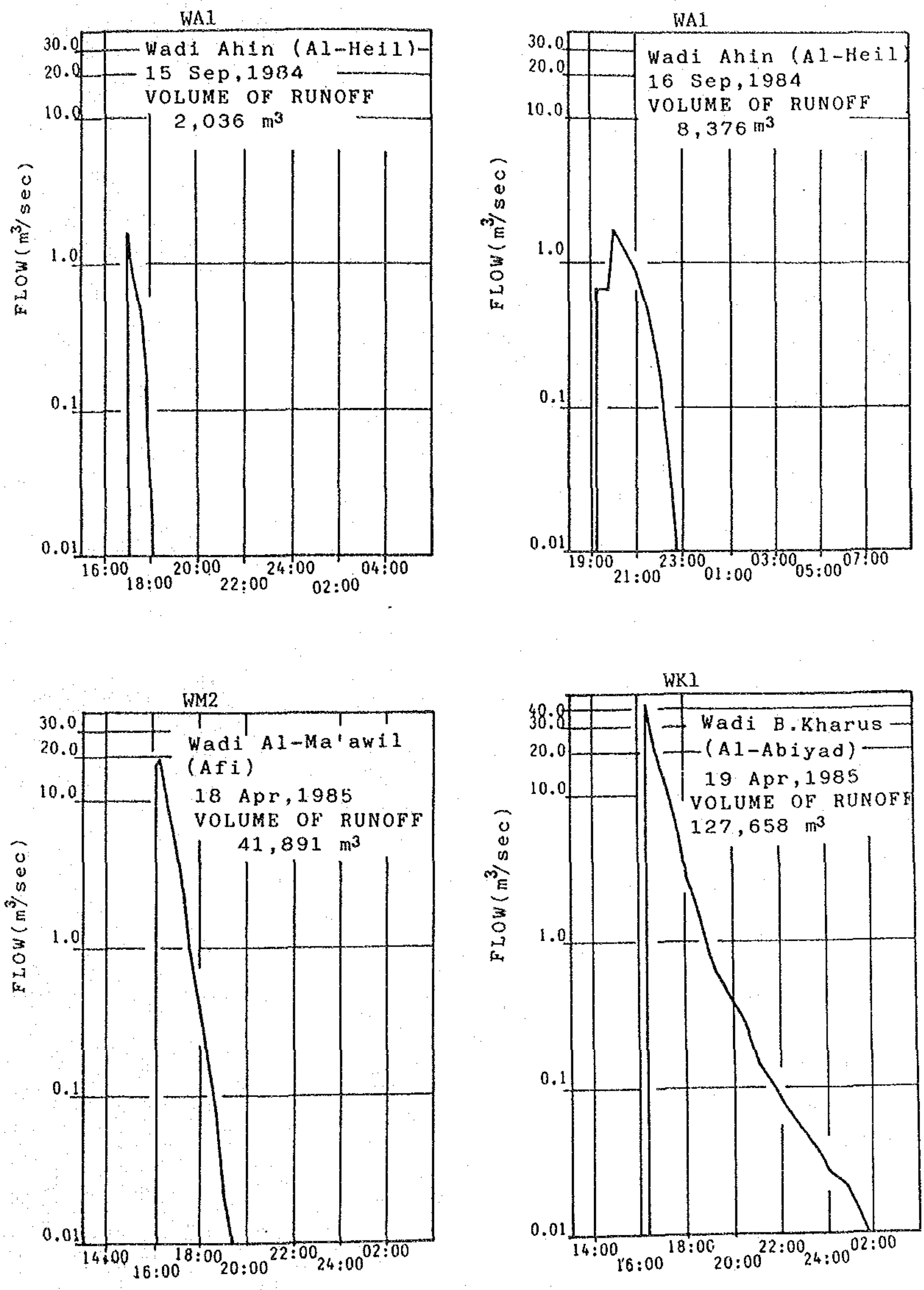

Fig. 4-2-14 Cross Section and Longitudinal Profile of Wadi Gauge Site (WG1)

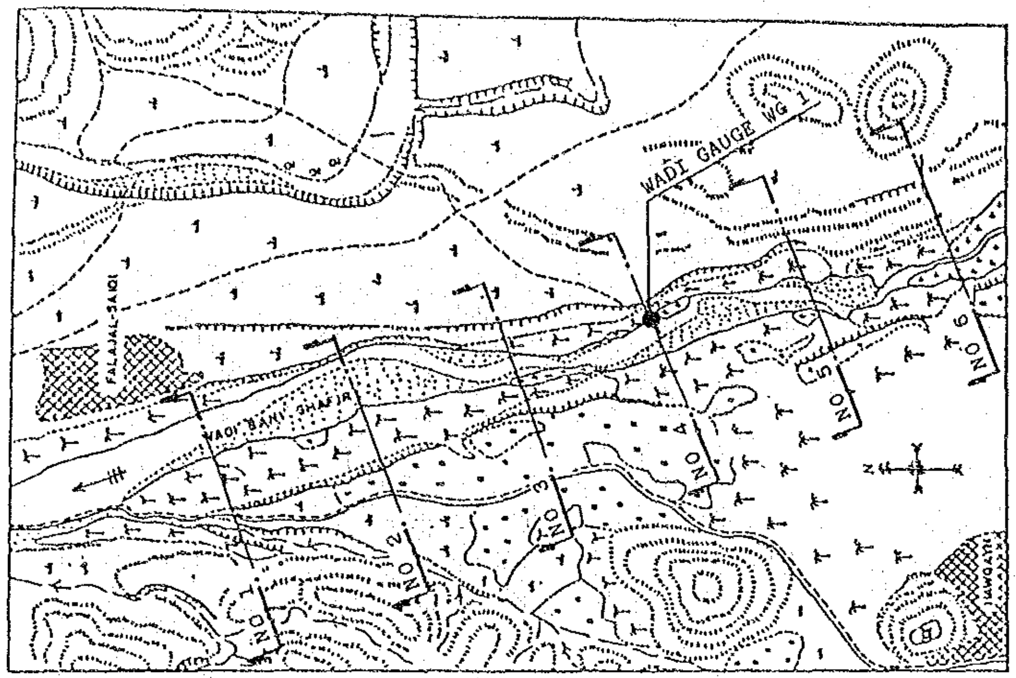

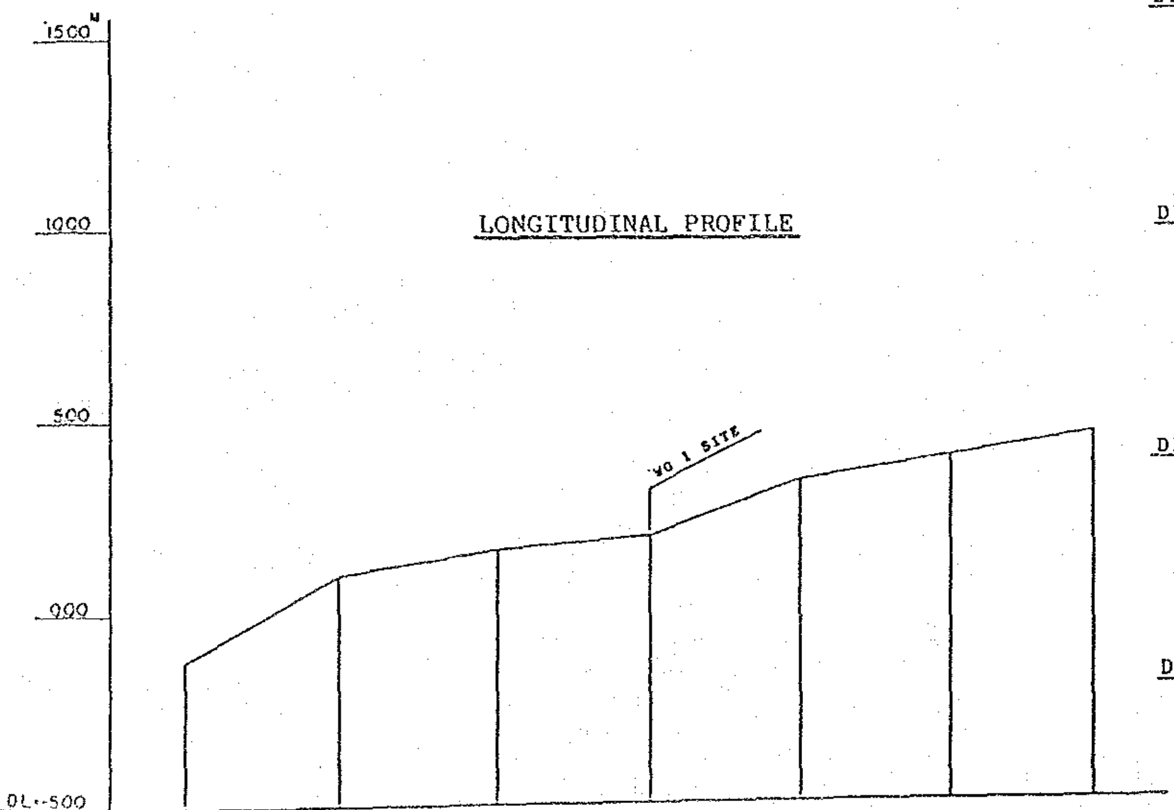

LONGITUDINAL SLOPE		0.985	I=1/249 L=600m		1.425	I=1/323 L=400m	2.665
PRESENT ELEVATION: RIGHT BANK							
PRESENT ELEVATION: LEFT BANK							
PRESENT ELEVATION: MEAN RIVER BED							
PRESENT ELEVATION: LOWEST RIVER BED	3.200	0.985	0.300	0.000	1.425	2.065	2.665
ACCUMULATED DISTANCE	0	200	400	600	800	1000	1200
DISTANCE	0	200	200	200	200	200	200
STATION No.	1	2	3	4	5	6	7

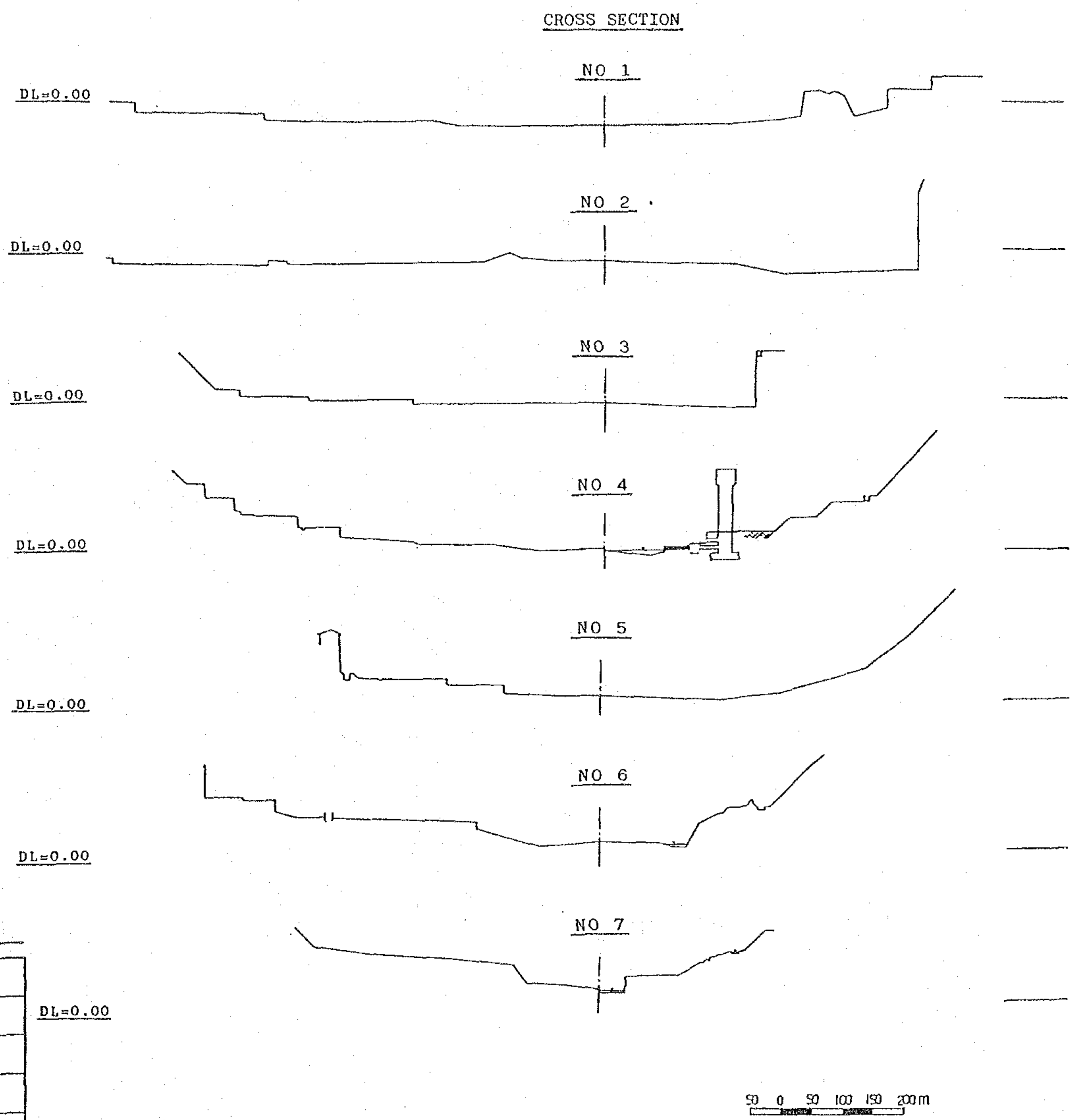

(2) Surface Runoff Features

It was observed that some rain, which caused runoff observed at the wadi gauges, were not recorded at the rain-gauges located in the same basins because of their small coverage. The density of the rain gauges will be reviewed after several years observation for the further improvement. Although the amount of data obtained during the Project is not large enough, the general relationship between rainfall and runoff are described based on these observation data and previous studies (ILACO and GIBB, 1977).

1. Short duration of runoff

The minimum duration of runoff was about 30 minutes and the maximum was about 24 hours. Hence, runoff can be said to be of very short duration usually.

2. Rapid runoff in the mountain area

The Project area is located in the semi-arid zone and has Major Mountains which are covered by steep bare rocks with sparse vegetation. These basin conditions causes the flood waters to reach Wadi bed in short time. In addition, wadi gradients are steep, ranging between 1/75 -1/145. These conditions cause rapid runoffs in the mountain areas.

3. High infiltration capacity of the wadi-bed

The rapid depletion of the hydrographs implies that the wadi-beds have a high infiltration capacity. Many instances of the rainfall were recorded at the rain-gauges in the mountain area, whereas no discharge was recorded at the wadi gauges downstream due to the wadi infiltration.

4. Floods of the coastal area occur mainly in winter

The number of the floods in winter is greater than the ones in summer in the coastal area. This tendency suggests that there is a relationship between the rainfall intensity and the infiltration capacity of the gravel plain. However, infiltration capacity varies widely in the coastal plain. High infiltration is available only among the wadi beds and in the zones of wadi termini, which occupy 1,000 sq. km in the coastal area of 2,700 sq. km. The rest of the coastal area is practically regarded as non-permeable.

4.2.4 Flood Discharge to the Sea

Flood discharge to the sea was not observed during the observation period (from Sept. '83 to Aug. '85). Flood discharges to the sea which had been observed in previous studies are summarized in Table 4-2-6. Those 7 floods occurred in the winters from 1974 to 1976. The year of 1976 had heavy rainfall according to the rainfall data of Muscat (See Table 4-2-7). From the previous studies and our observation, flood discharge to the sea is rare for the following reasons:

1. The wadi beds in the coastal area which are composed mainly of sand and silt have a large infiltration capacity. Consequently, most of the runoff infiltrated along the wadi bed.

2. Marginal wadi plain/Sand and Gravel Plain (2700 sq. km) spread out from about 10 km upstream of the seaside for about 35 km to the interior. The surface of the Maginal wadi plain area is cemented hard which will easily cause surface runoff. However, the wadi beds have a high infiltration capacity, which will accelerate the depletion of the discharge into the ground.

3. Major mountains are mainly covered with bare rocks and sparse vegetation. Surface runoffs occur easily, but the wadi-beds are covered with gravels where the surface flow can easily infiltrate.

Accordingly, surface runoff to the sea has only the following reference data:

Regarding the surface runoff to the sea in the Batinah area about 70 MCM/year was observed by Gibb, and Horn (1979) and Cardew (1980) reported that runoff to the sea is about 20-23 MCM/year (Table 4-2-8). The estimations by Horn and Cardew are very similar except for the discharge from Wadi Bani Kharus.

Table 4-2-6 Observed Flood Discharge to the Sea during Previous Survey Period

Wadi Basin	Name of Place (Name of gauge)	Runoff date	Runoff duration	Peak flow m^3/sec.	Amount of Runoff m^3
Wadi 1/ Ahin	Khishdah	Feb.15'74	No Data	1.2	12,000
		Feb.15'74	No Data	1.4	20,000
Wadi 2/ Bani Kharus	Al-Sawadi (N4)	May 14'75	17:45 - 02:00	3.4	74,506
		Feb.02'76	00:00 - 05:00	4.6	29,715
		Mar.25'76	02:00 - 03:30	1.2	6,720
		Mar.30'76	23:00 - 07:00	1.9	23,640
		Apr.09'76	02:30 - 06:00	6.9	51,900

Note: 1/ ILACO JUL. 1975
"WATER RESOURCES DEVELOPMENT PROJECT NORTHERN OMAN"

2/ SIR ALEXANDER GIBB AND PARTNERS JUN. 1976
"WATER RESOURCES SURVEY OF NORTHERN OMAN"

Table 4-2-7 Annual Rainfall at Muscat during Previous and JICA Survey Period

Year of Survey Period	Annual Rainfall (mm/year)
1974	3.7
1975	80.0
1976	203.3
1983	123.0
1984	18.5
Mean *	105.0

* Mean of rainfall data from 1951 to 1984

Table 4-2-8 Estimated Flood Discharge to the Sea for the Median Year

(Unit = MCM/year)

Reorters	Wadi Ahin	Wadi B. Ghafir	Wadi Al-Fara'	Wadi B. Kharus	Wadi Al-Ma'awil	Total
ILACO 1/	2.58	-	-	-	-	2.58
GIBB 2/	-	21.2	13.9	27.7	7.0	69.8
HORN 3/	5.5	4.5	4.1	5.4	0.4	19.9
CARDEW 4/	4.8	3.8	3.6	10.9	0.3	23.4

Note: 1/ ILACO JUL. 1975
"WATER RESOURCES DEVELOPMENT PROJECT NORTHERN OMAN"

2/ SIR ALEXANDER GIBB AND PARTINERS JUNE 1976
"WATER RESOURCES SURVEY OF NORTHERN OMAN"

3/ P.M. HORN-F.A.O. FEB. 1979
"WATER RESOURCES OF THE BATINAH"

4/ PRECCE CARDEW AND RIDER/SIR M MACDONALD AND PARTNERS SEP. 1980
"POWER AND URBAN WATER SUPPLY STUDY: PHASE II, WATER DEVELOPMENT PROGRAME"

Fig. 4-2-15 Observed Runoff to the Sea during Previous Survey Period

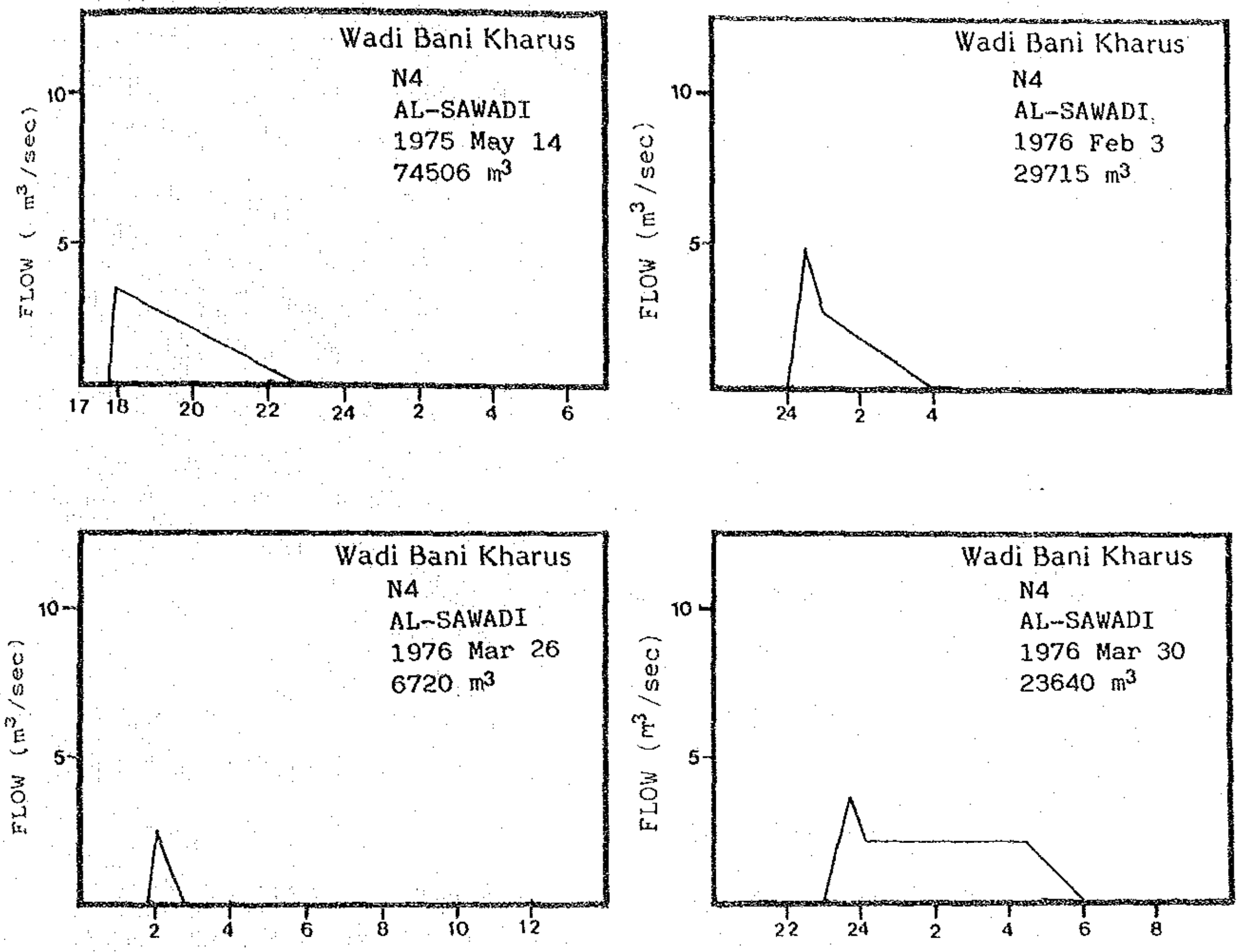

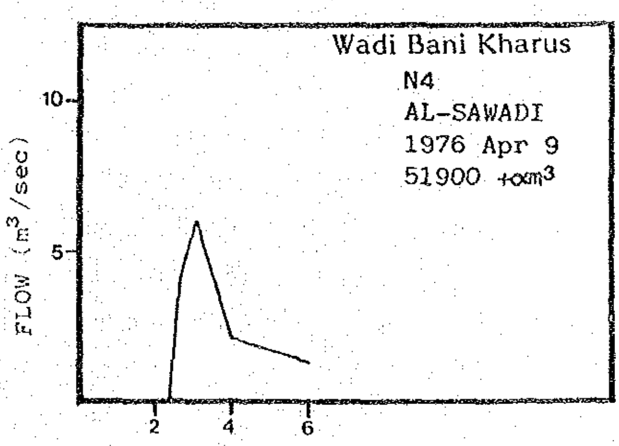

Note: Hydrographs from GIBB Report (1976)

4.3 Hydrogeology

4.3.1 General Features

Preceeding projects for water resources development in Northern Oman presented a hydrogeological concept where the study area was divided into two distinctive zones differentiated by the properties of the dominant geologic formation in each locality: Hard Rock Zone and Soft Rock Zone (Gibb, 1976).

Hard Rock Zone is made of well-consolidated rocks such as limestones and peridotites. These rocks are poor in water bearing property in general. Soft Rock Zone is covered mainly by clastic material such as alluvial deposit which is generally porous and forms aquifers. Thus the four geomorphological zones discussed in Chapter 4.1 are grouped into two hydrogeological zones introduced above: Major Mountains and Frontal Mountains are of Hard Rock Zone, and Marginal Wadi Plain and Sand/Gravel Plain are of Soft Rock Zone.

In Hard Rock Zone, dominant rocks of Major Mountains are metamorphosed siltstone and conglomerate, dolostone, dolomitic limestone, and limestone. Those of Frontal Mountains are ultramafic marine volcanics and gabbroic rocks of ophiolite.

In Soft Rock Zone, marlstone and sandy mudstone of Marginal Wadi Plain crop out with minor hard Palaeogene limestone. Modern clastic deposits cover Sand/Gravel Plain extensively.

As a general trend, the older the rock units are, the poorer the permeability and water bearing capacity of rocks are to be found. Intermitent fluvial activity, caused by rare rains, makes deep valleys in the mountains, dissects old fans and other alluvium at the mountain outskirt, and forms braided water courses in the alluvial plain. Some of the flood water originating from mountain rain may reach the coast and eventually discharge into the sea, but most of it is consumed in evapotranspiration and groundwater recharge during the downstream movement. Groundwater recharge rate varies depending on the infiltration property of the top geologic formation. Usually surface infiltration is excellent along wadi beds in the upstream zone and in the sand/gravel plain of the middle/downstream zone.

Extensive aquifers are not expectable in Major and Frontal Mountains due to the compactness of rocks and the disturbed structure related to the large anticlinal tectonic in the former and the up-thrusting structures in the latter.

In Marginal Wadi Plain, the geologic facies suggest stratifications of various hydroconductive beds. At its upstream edge, neighbouring Frontal Mountains, Tertiary rocks abut the underlying older formations and reduces their own sedimentary uniformity. Consequently in Marginal Wadi Plain aquifers do not extensively develop. However, in Sand/Gravel Plain groundwater is more promising than in the mountain regions. A schematic hydrogeological section is given in Fig. 4-3-1.

In the following sections identified aquifers, their characteristics and distributions are explained.

4.3.2 Aquifers

(1) Type of Groundwater Occurence

1) Fissure and cavern water

Fissure and cavern water may possibly be found in Hard Rock Zone. Fissure water is thought to be stored along the structural lines in the mountain basement rocks, but it has not been confirmed so far. Pre-Permian rocks of inland basins have not been regarded as promising for this aquifer. However, in the dolomitic limestone of Hajar Super Group, which surrounds the inland basins, joint systems are widely observed. LANDSAT images indicate several lineament sets which may accompany fissure zones (Fig. 4-3-2). In the Hajar limestone, solution channels or caverns may develop through the joints and fissures. Some well-known springs are found to issue from the small-scale caverns.

Hawasina Complex and Semail Ophiolites, overlying Hajar Super Group, also belong to Hard Rock Zone. Any indications for good aquifers in them have not yet been found. A few springs can be encountered there, and they may be issuing from fissures along structural lines.

Fig. 4-3-1 Schematic Hydrogeological Cross-section of the Batinah

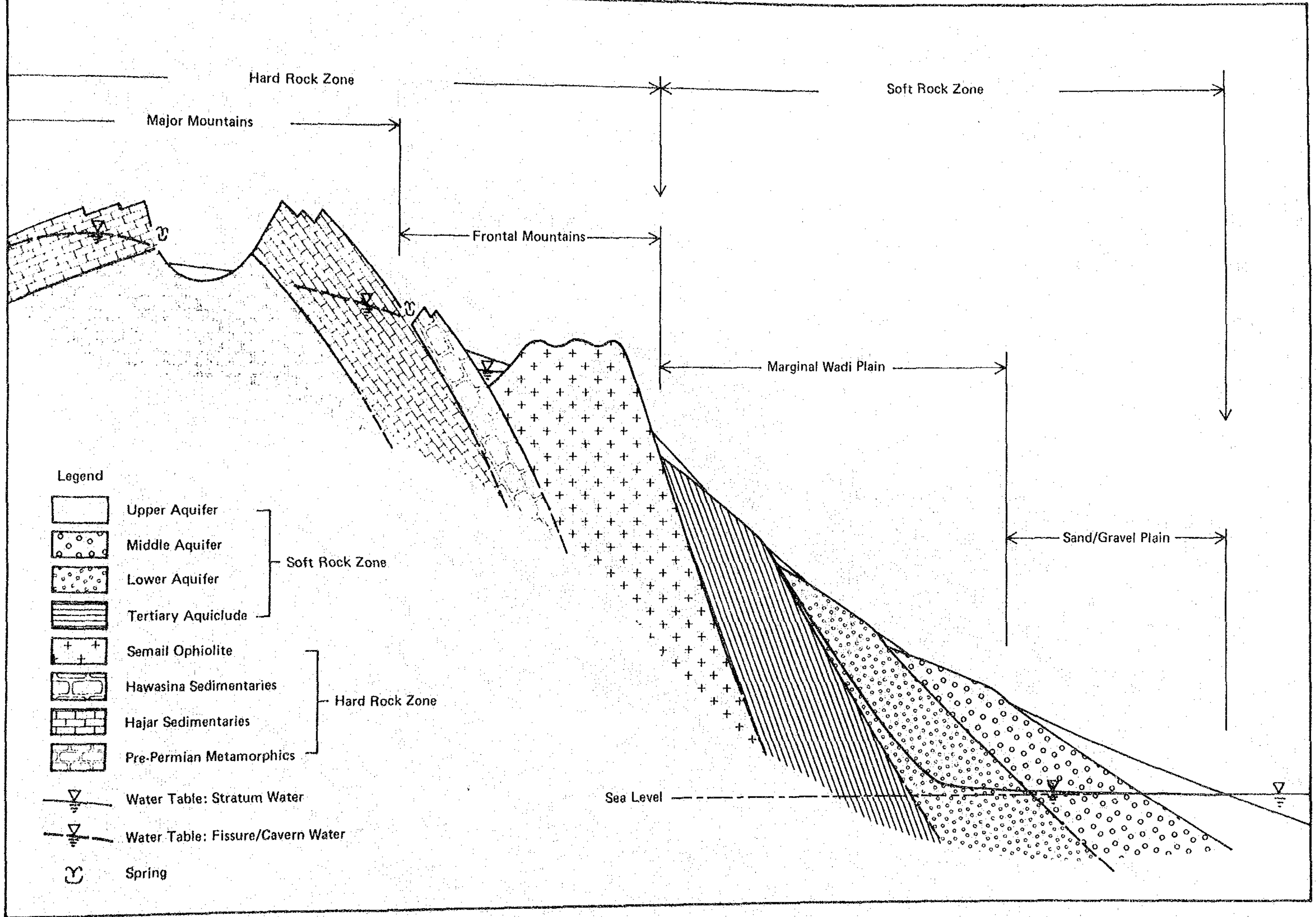

Fig. 4-3-2 Major Lineaments by the LANDSAT Imagery

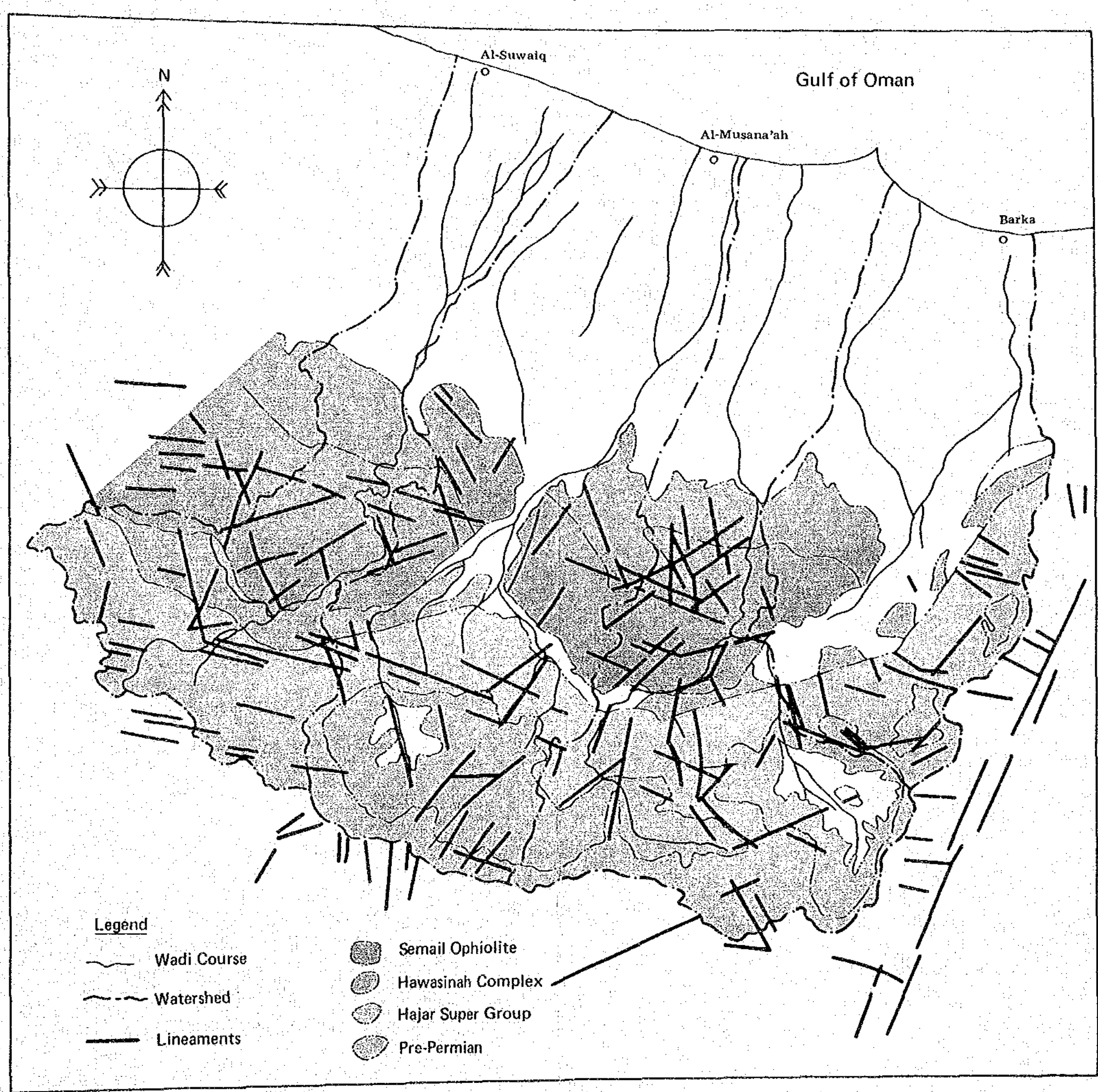

2) Stratum water

Stratum water exist in the Soft Rock Zone aquifers. Soft Rock Zone, consisting of deposits of Tertiary to Holocene, develops extensively in the coastal plain. However, some old terrace deposits extend deep into the upstream region and reach the level of 1,000 m approximately. They are small in scale in comparison with the coastal Soft Rock Zone deposits. Major Soft Rock Zone stretches from the periphery of Frontal Mountains to the coast, forming several series of deposits. The lower strata are of shallow marine limestone, marlstone and mudstone of Tertiary (Palaeogene). However, this limestone is an exceptional member in Soft Rock Zone and crops out linearly from north to south in parallel with the coastline. It has solution channels in some localities, but the scale of the aquifers of cavern water cannot be estimated.

Overlying Quaternary deposits can be characterized by the related alluvial terraces. The deposits of the upper terraces are sandy gravels cemented by limey mud. The lower terrace deposits and alluviums are not cemented. Stratum water is born extensively in the terrace deposits and the alluviums of the coastal plain.

The upper uncemented deposit is superior in aquiferous property to the lower cemented one. But near the coast the upper deposit becomes more silty and its water bearing property declines.

(2) Divisions of Aquifers

1) Hard Rock Zone (Major and Frontal Mountains)

In Major Mountains there are metamorphosed siltstones and conglomerates of Pre-Permian group cropping out in the Ghubrah (Wadi Bani Kharus) and the Sahtan (Wadi Al-Fara') basins. These rocks are often deformed and disturbed to a great extent and sometimes sustain fissure water. There are rather stationary groundwater discharges from these fissure water aquifers, but the amounts are not substantial. Some villages in the Sahtan basin are using this groundwater.

Late Palaeozoic/Mesozoic Hajar limestones provide springs in the two different levels of Major Mountains. One is at the contact level between

Hajar limestone and underlying Pre-Permian rocks, and the other at the boundary between Hajar limestone and overlying Hawasinah sedimentary group. Remarkably large springs are found in Al-Rustaq and Nakhal. In both localities springs issue from solution channels and their discharge does not fluctuate much over a long time span (cf. Fig. 4-3-9). These springs are usually exploited as the source of falaj.

Joints and fissures are observed widely in the limestone/dolostone area. These structure may have established fissure/cavern water aquifer in conjuction with the solution channels. In such case they may compose the most promising aquifers in Major Mountains, but at present details are not available. There is little prospect for good aquifers in the Hawasina sedimentaries and Semail ophiolite of Frontal Mountains.

2) Soft Rock Zone (Marginal Wadi Plain and Sand/Gravel Plain)

Clastic rocks are predominant in this zone. They date back to Palaeogene at the lowest stratigraphic level. Most of the available aquifers of this zone are stratum waters in the clastics. The clastics are differentiated by the texture, which reflect the facies and the diagenesis, and divided into three aquifer groups: Upper, Middle and Lower aquifers.

Upper Aquifer consists of gravels with sand layers and mainly develops in the lower coastal plain.

Middle Aquifer is made of silty gravels which are still not consolidated. This aquifer covers the mid to lower coastal plain.

Lower Aquifer's clastic formations are cemented gravels and muddy gravels. The coverage of this aquifer reaches almost all the area of the coastal plain.

These three major aquifer groups are underlain by the Tertiary fine clastics such as mudstone and marlstone. These Tertiary rocks are poor in aquiferous property and they are generally regarded as the aquiclude beds which form the basement rocks for the regional groundwater basin. However, there is a series of disturbed limestone beds in the lower level of the above-said formations. They may have aquifers in the fissures and the relatively porous beddings. Some of the villages, located near the

Palaeogene limestone outcrop in the upper part of the coastal plain, are utilizing this aquifer. This aquifer is presumably small in scale.

The Tertiary aquiclude beds extend coastward and descend more than 300 m near the coast. Regional isopach map of the aquiferous formation is not available due to the paucity of data concerning the depth to the Tertiary aquiclude beds. A summary of the aquifer division is presented in Table 4-3-1.

Table 4-3-1 Summary of Major Aquifers

Aquifer Division	Thickness	Geologic Period	Geologic Facies	Distribution in the Coastal Plain
Upper Aquifer	10 - 30 m	Holocene	Silt, Sand, Sandy Gravel	Lower Reach Coastal Strip
Middle Aquifer	20 - 60	Pleistocene Neogene	Sandy Gravel, Muddy Gravel	Mid/Lower Reach
Lower Aquifer	50	Palaeogene	Muddy Gravel, Concreted Gravel	Most of the Coastal Plain

(3) Hydraulic Property of Aquifers

Among the above-introduced aquifer divisions, only coastal aquifers have been explored for their hydraulic properties. Table 4-3-2 is the summary of the measured data in the project area. As most of the pumping tests were single well tests, the storage coefficients which are only obtainable by the multi-well tests, are not available in satisfactory number in the table.

Fig. 4-3-2 is a schematic diagram which suggests rough tendencies between the hydraulic coefficients and the aquiferous formations. It is worth noticing that each aquifer division has wide range of hydraulic properties. The measured coefficient varies by two orders in some aquifer divisions, e.g. Lower Aquifer.

Table 4-3-3 is the tentative classification of hydraulic properties prevailing in each aquifer division.

Table 4-3-2 Measured Hydraulic Coefficients and Division of Aquifers

Test Well No.		Specific yield (m^2/day)	Trans-missibility (m^2/day)	Permea-bility (m/day)	Stora-tivity	Aquifer Division	Watershed Basin
BA	1	1,630	1,950	21	-	Upper, (Middle / Lower)	Wadi Ahin
EA	5	5,060	5,380	141	-	Middle (Lower)	"
WSI	24	990	-	-	-	Middle	"
EA	3	1,230	2,580	61	-	Lower	"
EA	4	2,170	2,760	71	-	Lower	"
EA	6	30,000	2,120	56	$2.1x10^{-2}$	Middle (Lower)	"
JT	20A	108	59	25	$5.4x10^{-4}$	Lower	Wadi Bani Ghafir
JT	22	2,550	1,330	33	-	Lower	"
ADG	25	79	36	-	-	-	"
ADG	26	366	168	-	-	-	"
HT	1	2,330	-	-	-	-	"
HT	2	580	-	-	-	-	"
BG	1	612	2,050	72	$7.3x10^{-4}$	Middle	Wadi Al-Fara'
BG	2	3.7	0.9	0.04	-	Aquiclude	"
BF	1	1,790	1,850	21	-	Middle(Upper / Lower)	"
JT	13	1,030	473	4	-	Middle (Lower)	"
JT	15	1,020	468	13	-	Lower	"
ADG	20	183	84	-	-	-	"
JT	24	153	426	2	-	Lower	Wadi Bani Kharus
JT	57	562	204	7	-	Middle (Lower)	"
JT	58	247	72	1	-	Lower	"
JT	67	694	220	15	-	Lower	"
JT	69	533	316	3	-	Middle (Lower)	"
ADG	24	104	48	-	-	-	"
ADG	23	333	333	-	-	-	"
JT	11	45	14	1	-	Lower	"
JT	12	19	4	0.2	-	Aquiclude	"
JT	23	1,190	547	10	-	Lower	"
BM	1	588	-	-	-	Upper (Middle / Lower)	Wadi Al-Ma'awil
BM	3	823	269	9	-	Middle	"
JT	5	12	1	0.4	-	Lower	"
ADG	17	318	146	-	-	-	"

Note: Aquifer division in parentheses has some contribution.

Fig. 4-3-3 Schematic Diagram for Hydraulic Coefficients vs. Aquifers in the Coastal Plain

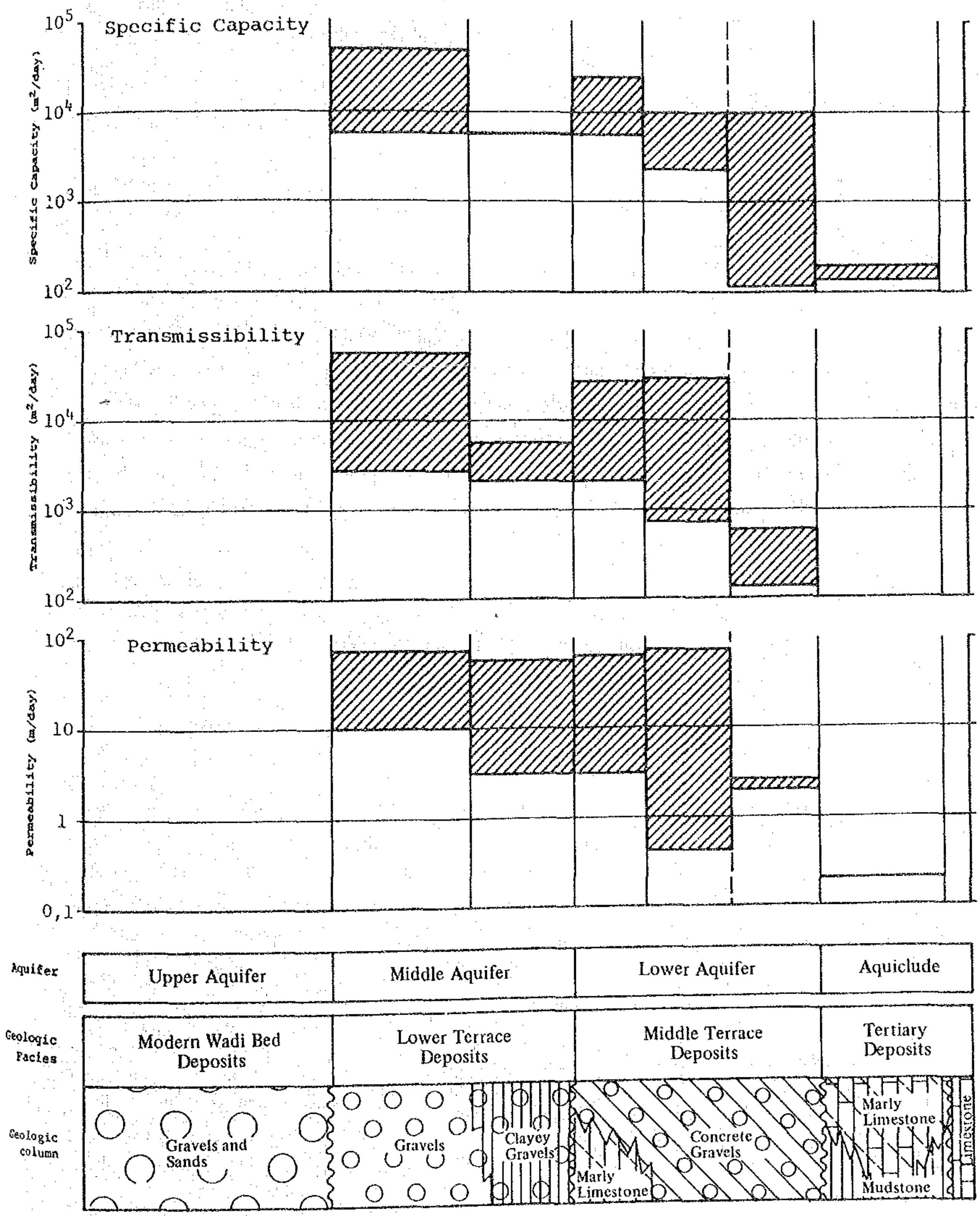

Table 4-3-3 Tentative Classification of Hydraulic Property for Aquifer Division

Aquifer Division	Specific Capacity (m^2/day)	Transmissibility (m^2/day)	Storativity (%)
Upper Aquifer	7000 -	7000 -	2
Middle Aquifer	800 - 9000	350 - 9000	0.5
Lower Aquifer	100 - 3000	20 - 1000	0.3

(4) Characteristics of Aquifer Structure in Each Wadi Basin

As summarized in Table 4-1-3, four geomorphological zones divide each wadi basin in different ratios. Accordingly there are different hydrogeological structures characteristic for each basin. Hydrogeologic situations have not been intensively surveyed yet, so detailed differentiations of aquifer structure are not possible at this stage. Based on the relatively large number of exploration wells in the coastal plain, aquifer structure is estimated in reference to the identified three aquifers. Cross-sections of coastal aquifers are presented in Supporting Report C. Table 4-3-4 is the summary of the thickness of each aquifer division estimated for the coastal plain of each basin.

Table 4-3-4 Estimated Thickness of Aquifer Division in the Coastal Plain

(unit = m)

Watershed Basin / Aquifer Division	W. Ahin	W.Bani Ghafir	W. Al-Fara'	W. Bani Kharus	W. Al-Ma'awil
Upper Aquifer	10	30	15	30	25
Middle Aquifer	40	50	60	35	35
Lower Aquifer	>80	>100	>100	>50	>100

4.3.3 Dynamic Characteristics of Aquifers

(1) Groundwater Table

Using the mean annual water level of each coastal observation well, the total number of which is 49, a regional groundwater level map was drawn for 1984. The map (Fig. 4-3-4) shows two apparent ridges of the water level contours in the southern four wadis basins. One of the ridges lies around the watershed boundary between Wadi Bani Ghafir and Wadi Al-Fara'. The other extends along the major Wadi bed of Wadi Bani Kharus. The former seems to coincide with the old major alluvial course as if groundwater still prefers the past passages which are detached from the present major wadi flood infiltration. However, actual connection between the groundwater at the contour ridge and the major wadi base flow is not clear. The four coastal wadi drainages seem to underlie three groundwater flow systems divided by these two flow ridges.

The unique change of hydraulic gradient at the mid plain has been noticed by the preceding ground water surveys. Our results present some more precise patterns for this, based on the levelling survey of the observation wells utilizing the most recently established benchmarks. The hydraulic gradient concentrates in two ranges which characterize the localities.
In the lower half of the coastal plain the gradient is gentle (1/2500 - 1/1500), but in the upper half it becomes steep (1/500 - 1/300). The change is relatively abrupt, so the local geologic structure may induce the matter. The changing zone roughly coincides with the position where the coastwardly dipping Tertiary aquiclude beds reach the sea level (cf. Fig. 4-3-1), 20 km inland from the coast. This Tertiary aquiclude beds were extensively detected by the resistivity surveys throughout the coastal region. However, some unknown structural disturbance like fault could cause this unique trend of hydraulic gradient.

In order to clarify the details of the seaward hydraulic trend of the groundwater, a series of levellings both for ground levels and water table levels was carried out. Five traverse lines were chosen near the major wadi courses at the coast so that the groundwater runoff to the sea could be visualized by the cross-sectional diagram of the coastal water table.

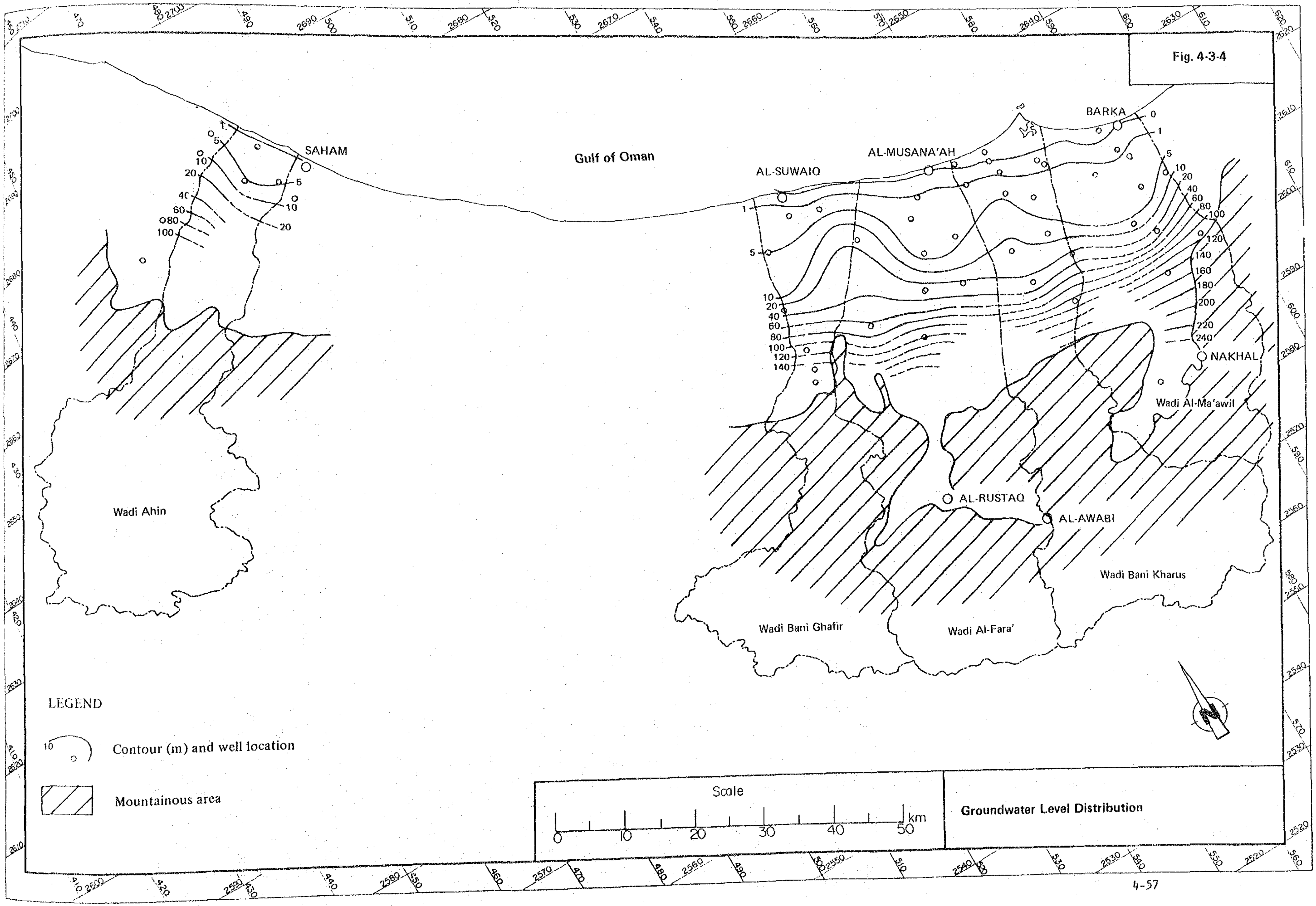

Fig. 4-3-4
Gulf of Oman
SAHAM
AL-SUWAIQ
AL-MUSANA'AH
BARKA
NAKHAL
AL-RUSTAQ
AL-AWABI
Wadi Ahin
Wadi Al-Ma'awil
Wadi Bani Ghafir
Wadi Al-Fara'
Wadi Bani Kharus
LEGEND
Contour (m) and well location
Mountainous area
Scale
0 10 20 30 40 50 km
Groundwater Level Distribution

Fig. 4-3-5 Cross-sectional Profile of Ground and Groundwater near the Coast

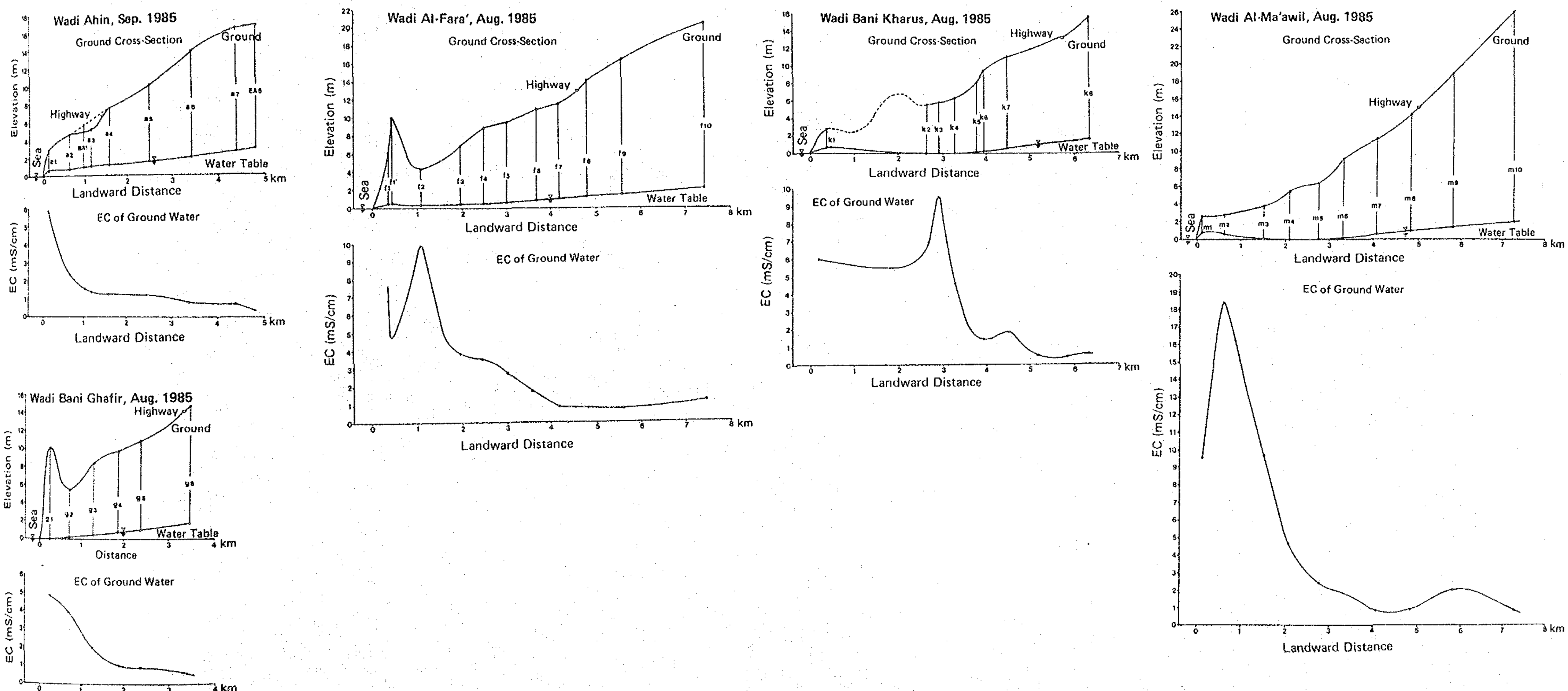

note: Locations are given in Appendix F, Hydrogeologic Map of the Batinah.

Table 4-3-5 Cross-Sectional Profile of Coastal Groundwater

Station No.	Distance from Coast (m)	Ground Level (m.a.s.l.)	Water Level (m.a.s.l.)	EC (25°C) (ms/cm)
W. Ahin				
a1	140	2.76	0.60	5.86
a2	650	4.46	0.74	2.35
BA1	990	5.41	0.94	1.61
a3	1,170	5.06	1.01	1.37
a4	1,620	7.40	1.11	1.26
a5	2,520	9.86	1.42	1.21
a6	3,450	13.57	1.97	0.81
a7	4,380	16.05	2.45	0.72
EA5	4,810	16.42	2.89	0.34
W. Bani Ghafir				
g1	260	10.05	0.07	4.85
g2	730	5.43	0.25	3.93
g3	1,320	8.18	0.48	1.79
g4	1,900	9.87	0.83	0.92
g5	2,410	10.89	1.21	0.85
g6	3,470	14.28	1.86	0.47
W. Fara'				
f1	370	6.13	0.48	6.83
f1'	440	10.04	0.54	4.83
f2	1,070	4.33	0.37	9.88
f3	1,950	6.86	0.41	3.80
f4	2,480	8.94	0.50	3.51
f5	3,050	9.59	0.64	0.91
f6	3,700	11.09	0.87	1.58
f7	4,180	11.73	1.02	0.88
f8	4,800	14.37	1.23	0.83
f9	5,580	16.76	1.50	0.77
f10	7,440	21.00	2.27	1.23
W. Bani Kharus				
k1	390	2.77	0.67	5.90
k2	2,650	5.44	0	6.34
k3	2,910	5.72	0.02	9.55
k4	3,290	6.17	0	4.57
k5	3,790	8.04	0.14	1.61
k6	3,960	9.42	0.27	1.44
k7	4,500	10.83	0.55	1.83
k8	6,340	15.48	1.63	0.60
W. Al-Ma'awil	120	2.59	0.76	9.55
m1				
m2	630	2.79	0.59	18.34
m3	1,530	3.74	0.14	9.60
m4	2,100	5.46	0	4.65
m5	2,760	6.41	0.02	2.43
m6	3,330	9.04	0.17	1.88
m7	4,080	11.42	0.50	0.84
m8	4,840	14.26	0.94	0.89
m9	5,820	18.84	1.47	2.05
m10	7,280	26.09	2.06	0.76

Fig. 4-3-5 and table 4-3-5 show a set of the results. Except for two wadi drainages in the north, three wadis have remarkably depressed water tables before reaching the shore. At the depressed zone, groundwater EC has significantly high value. The EC decreases seaward from this zone, being accompanied by the recovering groundwater level.

The recovering water table reaches maximum at the seaside sand dune zone. So the sand dune may provide groundwater recharge from the local precipitation and/or the intercepted wadi floods. Also, there may be some recharges from the domestic water discharge of the villages on the dune.

This coastal hydraulic structure presumably develops widely, so the groundwater makes only a few direct runoffs to the sea. Our survey results reached the same conclusion that was derived by the preceding surveys on the basis of extensive sabkhah distribution inside of the coastal sand dunes.

(2) Fluctuation of Groundwater Level

1) Long Term Changes and Their Geographical Variation

Long term well-hydrographs (1976-1984) are compiled in the Hydrogeologic Map (Appendix F) and Supporting Report C. Two types of hydrograph seem to occur: large-range fluctuation prevails in the steep hydraulic gradient zone in the upper sand/gravel plain, and small fluctuation in the gentle gradient zone in the lower plain. In 1976 - 1984 most of the large fluctuations were characterized by two peaks which exceed 5 meters over the lowest level.

Among these hydrographs, some of them recorded quite large annual change which exceeded 10 meters (Fig. 4-3-6). In the figure JT14 well hydrograph shows surprisingly steep change which happened after almost a decade-long dryness at the bottom. These steep and large changes usually takes three to six month. In case of JT7, both increasing and decreasing of water level happens at a similar high rate.

However, the gentle fluctuation zone sustained secular decrease of water level by 2 m approximately which was presumably caused by the intensified pumping for irrigation in recent years.

2) Distribution of Annual Water Level Increment

Fig. 4-3-7 shows the distribution of annual increment of groundwater level. Besides the result of JICA (1984), the result of Gibb (1974) is presented for reference. There are two plus increment zones in our result which almost coincide with the positions of groundwater ridges discussed above. Gibb's result does not have two clear zones, but it indicates a similar tendency. The annual increments are greater in 1984 than in 1974. We could not detect simple overall decrease of groundwater level in the coastal plain.

3) Daily Change, Observed in Recorded Charts

Twenty automatic water level recorders were used in the project area. Their recorded hydrographs show quite interesting patterns which can be classified into several types. Fig. 4-3-8 (1) shows six typical examples. A tentative classification is given in Table 4-3-6.

Fig. 4-3-6 Typical Large Fluctuation of Groundwater Level (JT7, JT16, JT14)

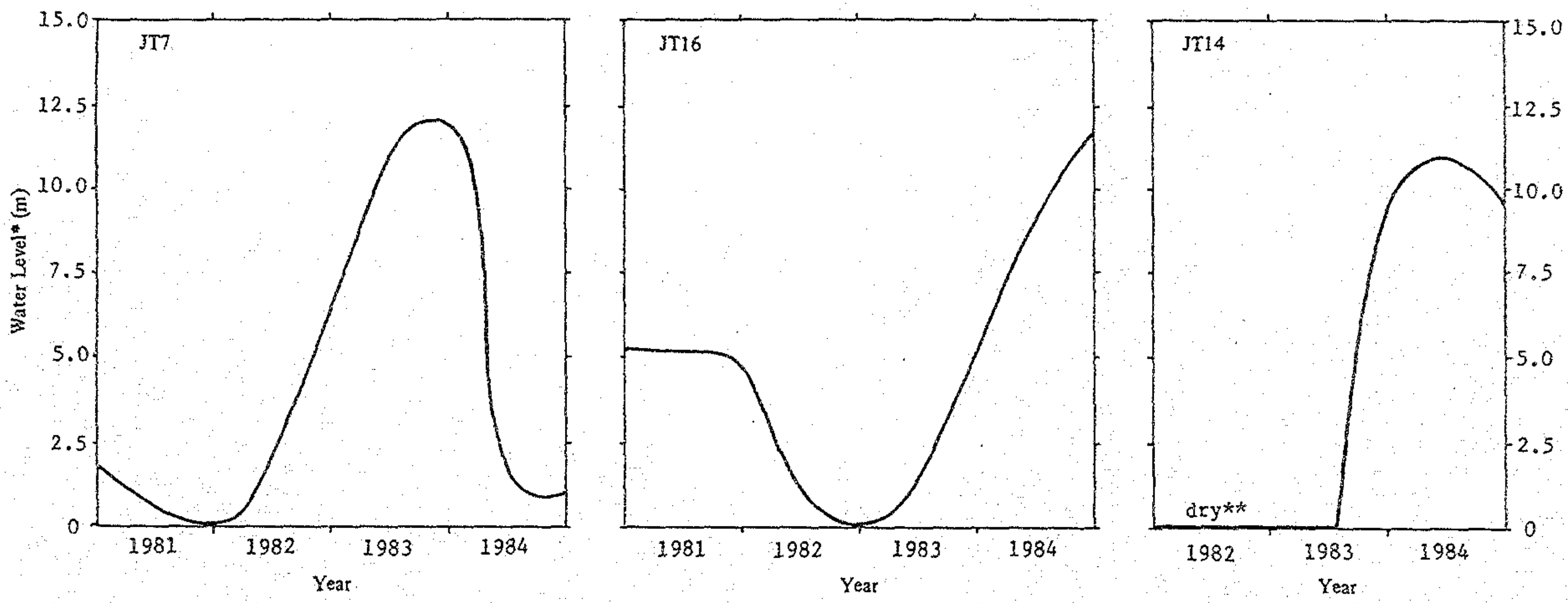

* Increment from the lowest level
** Stayed dry since establishment (1974)

Fig. 4-3-7 Distribution of Annual Change in Groundwater Level

Gibb (1974)

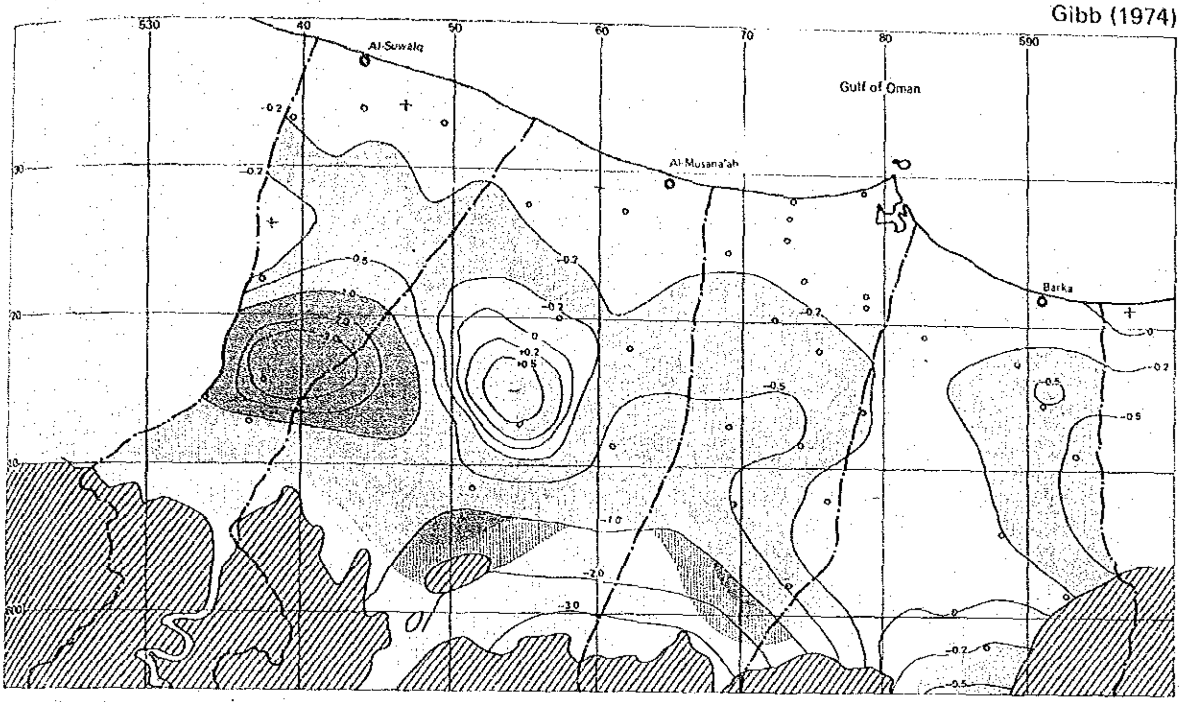

JICA (1984)

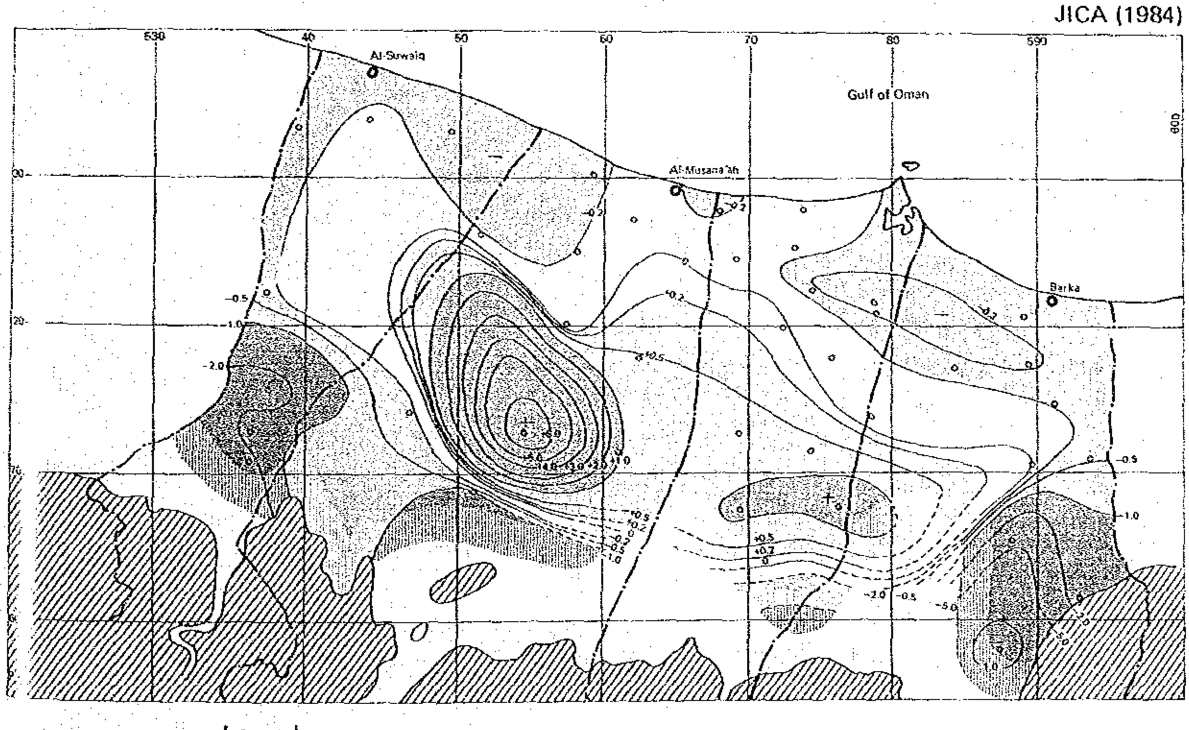

Legend

Watershed

◎ Barka Town with name

o Observation point

Exposed rock area

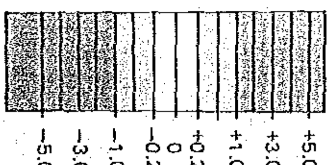

Fig. 4-3-8 (1) Typical Variation Patterns of Groundwater Hydrograph

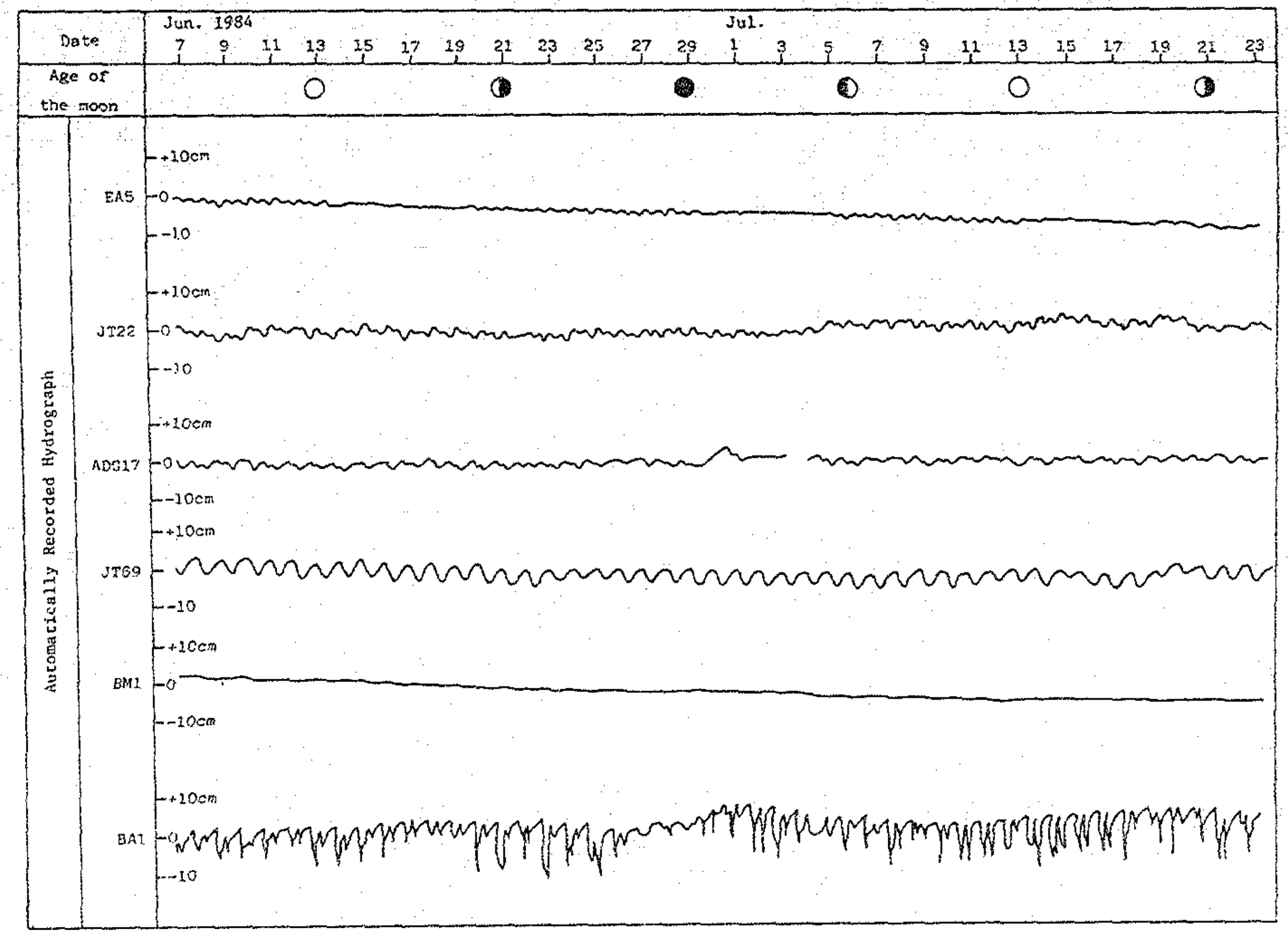

Table 4-3-6 Classification of Well Hydrograph

A. Pulse type A1. Single daily pulse type
A2. Dual daily pulse type — A21. Beating type
A3. Multi daily pulse type — A22. Non-beating "

B. Non-pulse type

Type of Hydrograph	A				B
	A1	A2		A3	
		A21	A22		
Well No.	JT69	EA5	JT22	BA1	BM1
	JT19	JT10	JT67		BF1
		JT12	ADG17*		BG1
		JT15	ADG23*		JT9
					JT17
					ADG25
					JT52
					JT56
					(ADG17)

* non-symmetrical pulse form.

As an initial bifurcation, there are pulsing hydrographs (Pulse type (A)) and non-pulsing hydrographs (Non-pulse type (B)).

The pulsing hydrographs are differentiated into single daily pulse type (A1), Dual daily pulse type (A2) and Multi daily pulse type (A3). Dual daily pulse type consists of Beating type (A21) and Non-beating type (A22). The Pulse type hydrographs can also be divided into Symmetrical pulse type and Non-symmetrical pulse type. However, we avoided this last criterion for a conventional reason. Among twenty recording wells (one of them has been dry for long time), nine wells belong to Non-pulse type (B).

Among the rest, eight wells are Dual daily pulse type (A2). Half of them, i.e. four wells, are identified to be Beating type (A21). By the way ADG17 changed its hydrograph pattern and transfered to Non-pulse type. The details of the transfer will be explained later.

Although the pulse generation in the hydrograph is not clear, Dual daily pulse type has some similarity with the hydrographs influenced by the earth tidal force (cf. Nilsson, L. Y., 1965, Tellus, Vol. XVII, pp 403-404).

Especially the Beating type has identical properties with the earth tidal phenomena in which the beating follows the cycle of the age of the moon. But dual daily pulsing is also explainable by the daily two pumping peaks prevailing in the agriculture field. However, sensitive wells respond with sharp multi-peaks to the local pumpings (BA1). For the satisfactory understanding of these phenomena, more observation wells should be drilled and more continuous recording charts should be collected.

As mentioned above, ADG17 transfered from type A21 to B during the observation period. The details are shown in Fig. 4-3-8 (2). ADG17 is quite similar with ADG23 both in hydrographic type and hydrogeologic location.

However, when the water levels decreased in ADG17, this well lost pulse waves and shifted to B type.

An interesting phenomena happened when local farmers stopped irrigation and recessed pumping due to the Islamic Holidays (Idd Al-Fitr and Idd Al-Adha). During the recess, local water level recovered to some extent, then the well resumed the former Pulse type hydrograph. The pulse waves in the hydrograph seem to be enhanced when the hydraulic pressure increased. This means that ADG17 taps a piezometric aquifer which receives injective water supply from another deep born aquifer. The injection may be driven by the earth tidal force. In this context ADG23 is regarded to have enough piezometric pressure so that dual daily pulsing is intact.

4) Change of Falaj Discharge

Falajs utilize various water sources. As most falajs are located in the mountain area, so the change of their discharge may disclose some hydrogeologic properties of their water source. Fig. 4-3-9 is a long term record of several falaj discharges which include spring falajs and ordinary wadi bed falajs.

Fig. 4-3-8 (2) Hydrograph of ADG17 and ADG23

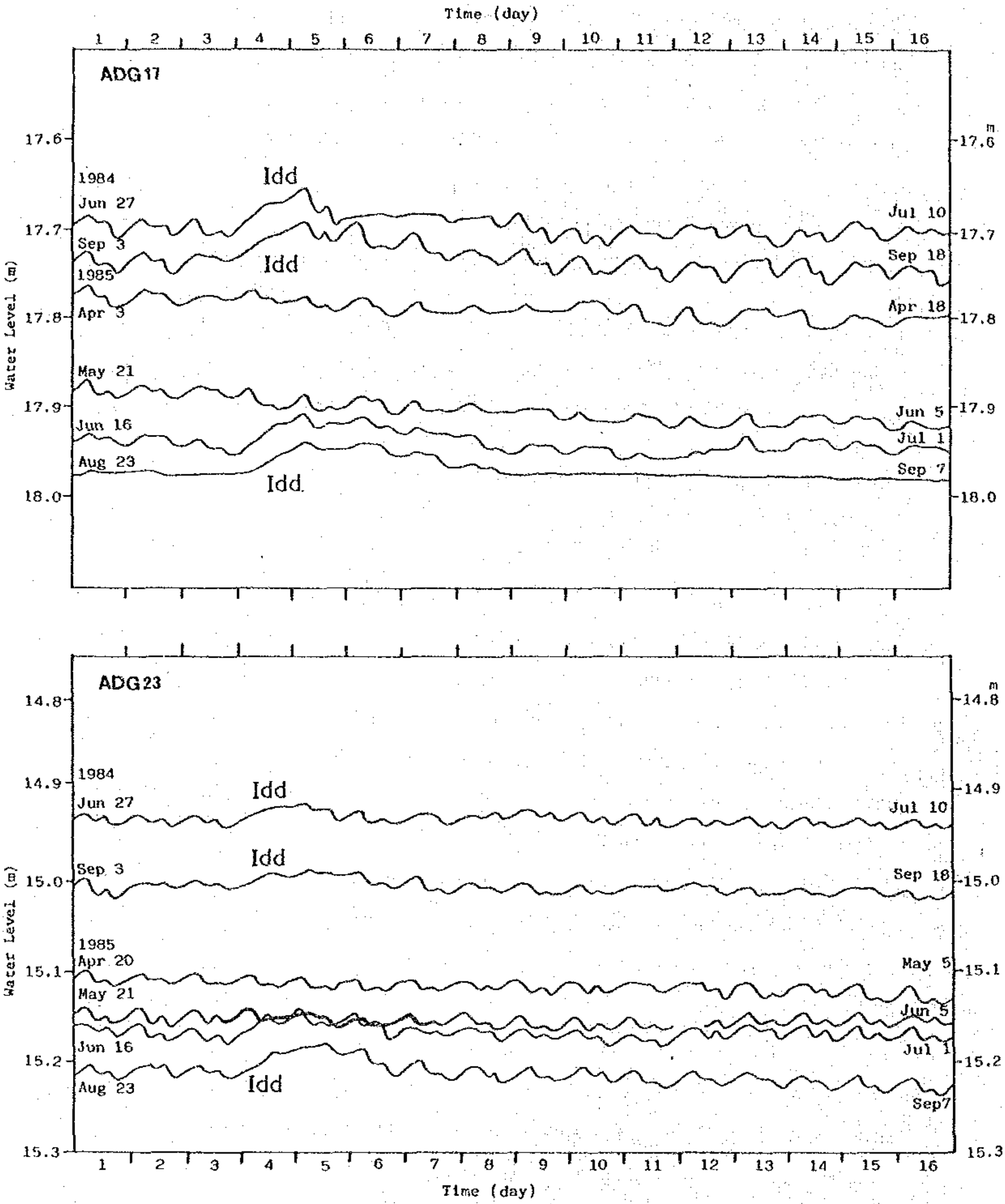

Fig. 4-3-9 Change of Falaj Discharge

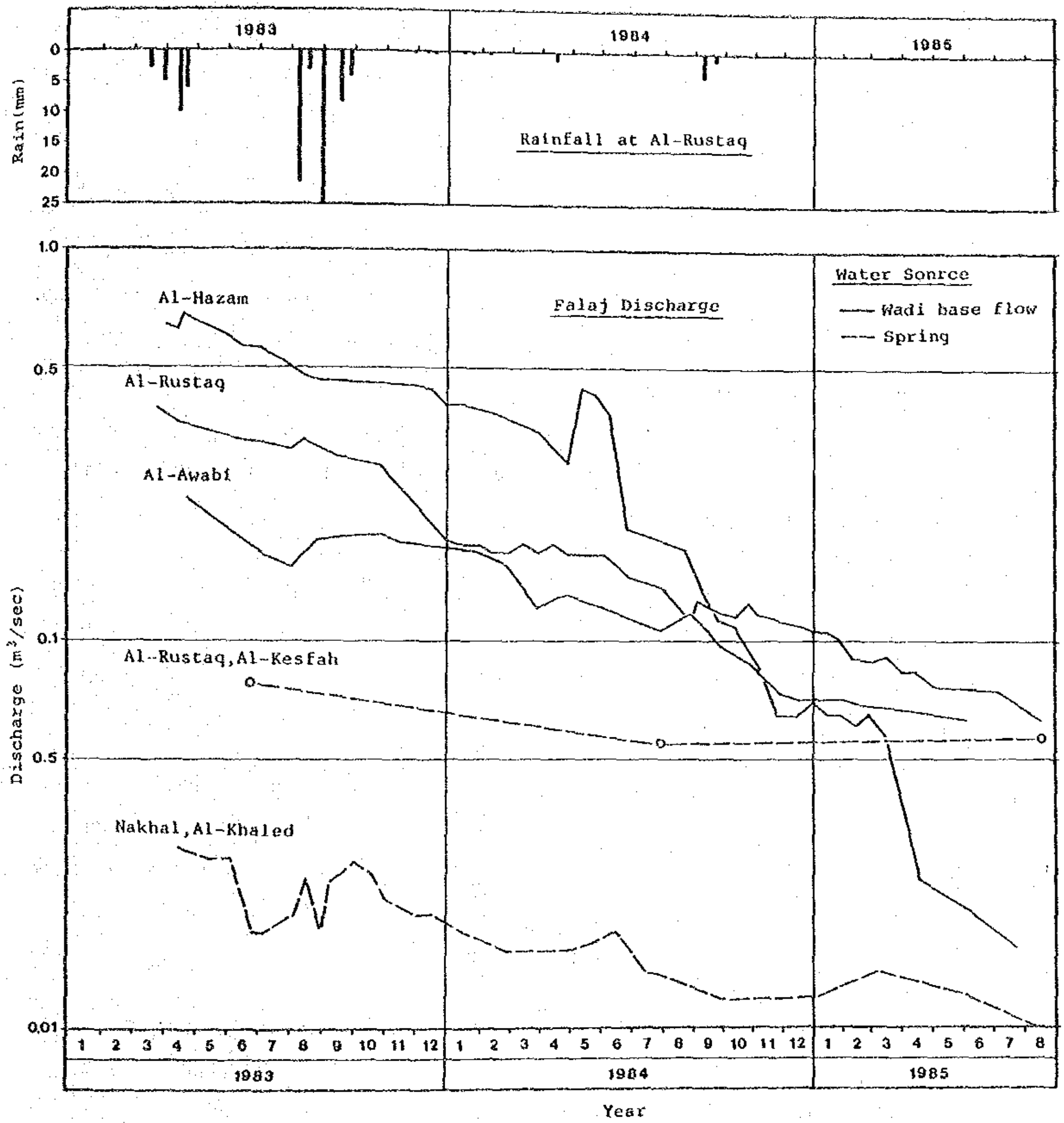

There is steady decline in most of the falajs presented in the figure. Falajs of wadi bed had diminished discharge to almost 1/10 in the 1983-1985 period. However, spring falajs made gradual decrease in discharge and one of them stayed at the stationary discharge level. The spring falaj may discharge a large reservoir which may be in the mountain limestone. On the other hand falajs of wadi bed have large discharges, but their rapid decline indicate relatively small groundwater storage in wadi bed.

5) Salt Water Interface of Groundwater

Aquifer intensity usually reflects in the level of salt water interface in the coast. The interface level shifts upside in a quite sensitive way when the aquifer looses its fresh water thickness: the decline of transmissibility. Due to the recent development of cultivated farms in the coastal region, the coastal aquifer is extra-intensively pumped up. So there is an increasing danger where the fresh groundwater reduces it thickness or sustains salt water mixing.

In order to detect any tendencies of the up-shifting of the salt water interface, two analyses were made: one is area analysis for the landward advance of salt water, and the other is vertical probe of the interface ascension.

For the area analysis, two EC surveys of the coastal groundwater; Gibb (1976) and MAF (1983) were used. Fig. 4-3-10 (1) and (2) are the results of the analyses. In Fig. 4-3-10 (1) 5,000 μs/cm contours of the two surveys were presented on the same map. 5,000 μs/cm contour is usually used to find the mixing front of salt water.

In the map two contours are found to cross each other at several points, so there was not overall advance of salt water in the analyzed Al-Suwadi region. Fig. 4-3-10 (2) was drawn to show the change of EC values at the same groundwater spot. The increase in EC value attains +6,000 μs/cm (1975-1983), but decrease is only -2000 μs/cm.

In conclusion, there was not considerable landward encroachment of salt water, but in some coastal spots, EC increased steeply.

Fig. 4.3.10(1) Change of 5,000 μs/cm EC Contour between 1975 and 1983

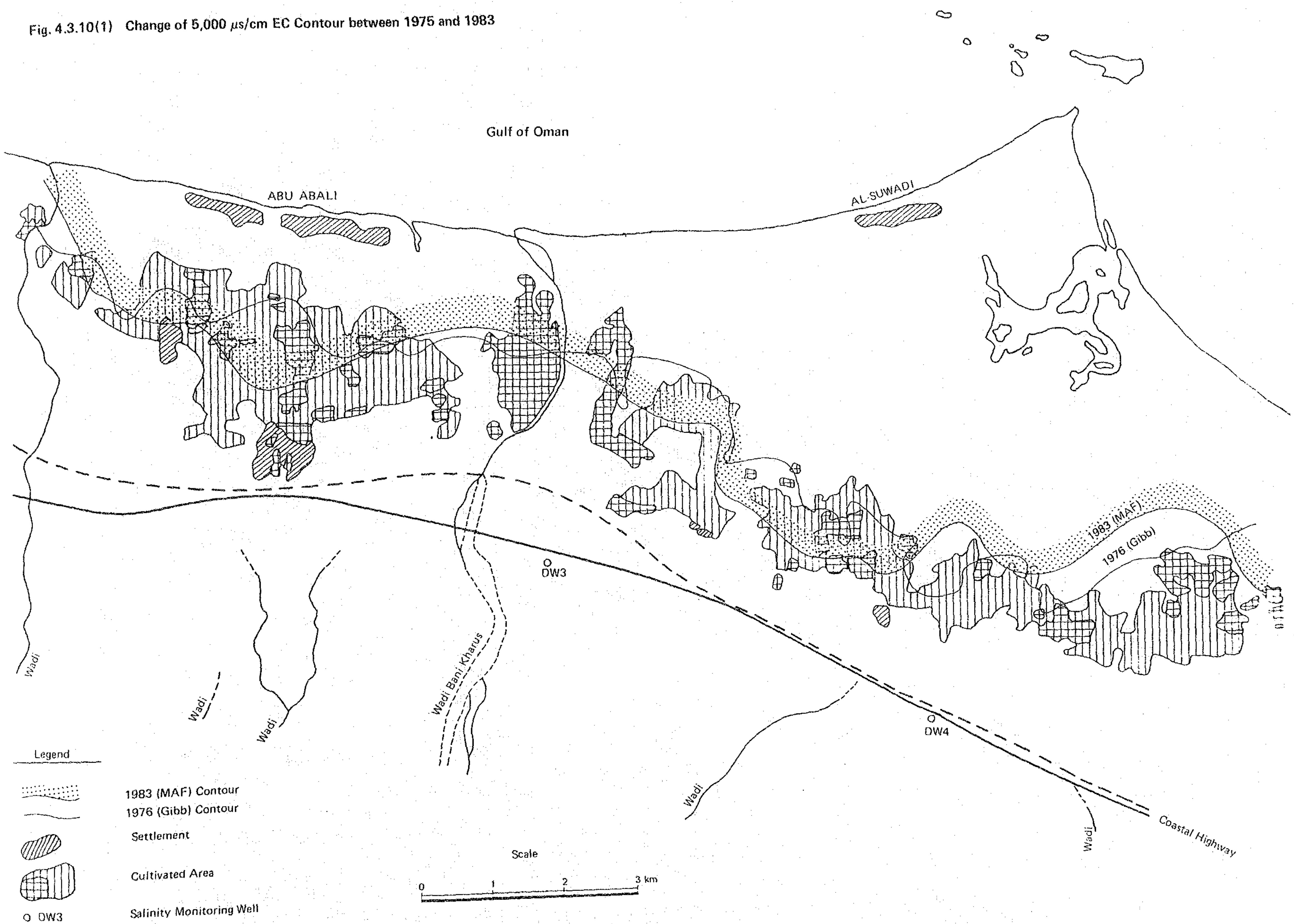

Fig. 4-3-10 (2) Distribution of EC Change (ΔL) between 1975 and 1983 in the Shallow Wells
(ΔL = L1983 – L1975)

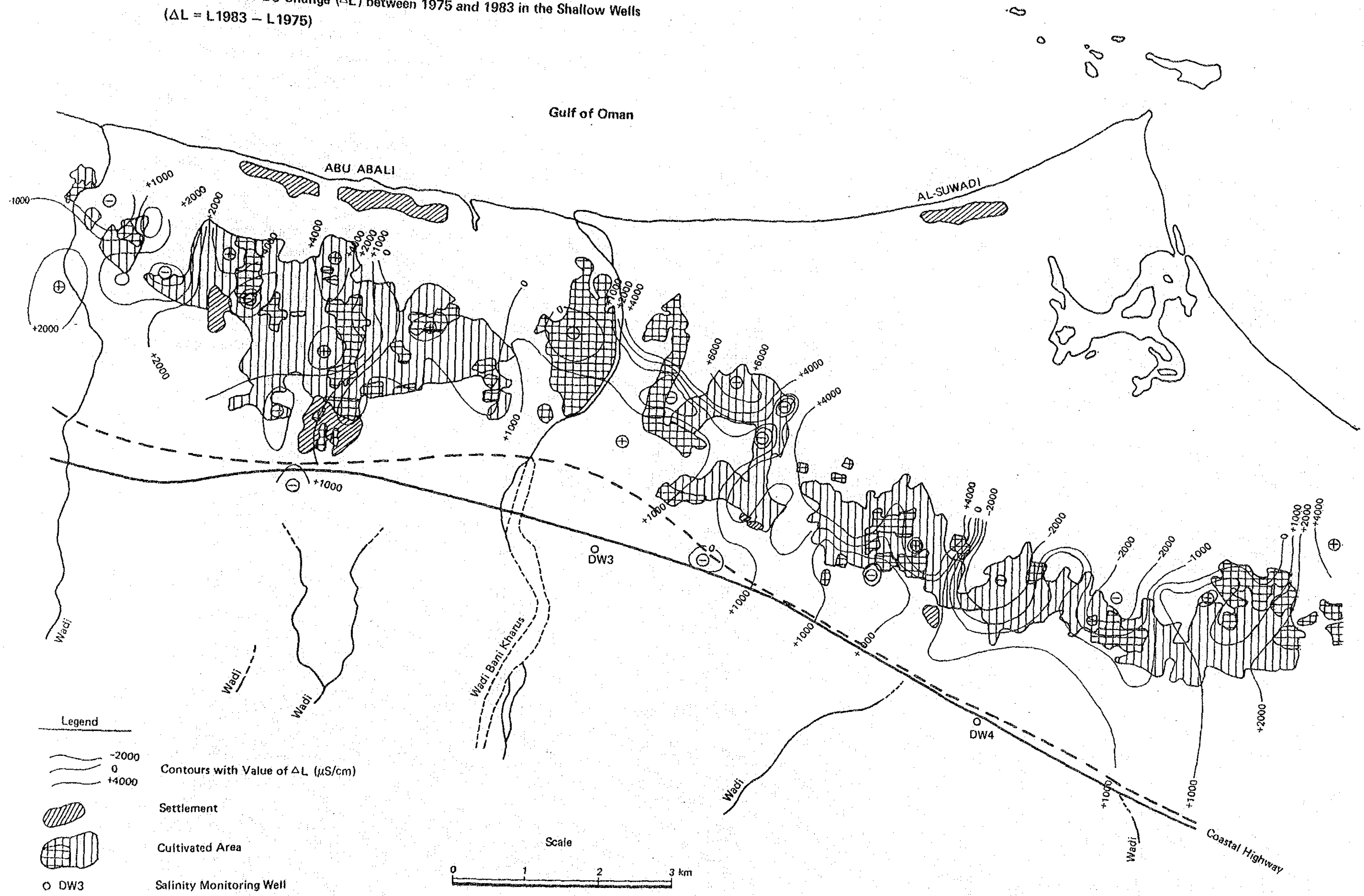

In order to clarify the vertical movement of salt water interface, we tried to determine the differences of salt water interface levels for a time interval (1976 - 1985), using DW3 and DW4 monitoring wells. Fig. 4-3-11 shows the results. Although there are differences of EC values, the log curves have quite identical patterns where the interface levels are located at the same positions.

In Fig. 4-4-12 (1) to (3) summaries of fourteen months EC monitorings of newly established wells are presented. These wells: BA1, BF1 and BM1, are each 100 m deep.

Since their establishment, EC logs have been carried out almost once a month. These three wells provided three different aquifer structures. Among them, only BA1 seems to have an aquifer where sea water actively intrudes from the bottom. The correlation coefficient (r) between the groundwater level and the interface level was r = -0.885. The interface in BA1 shows an ascending tendency of 0.734 m/yr.

Fig. 4-3-11 EC Log Changes in DW3 and DW4 between 1975 and 1985

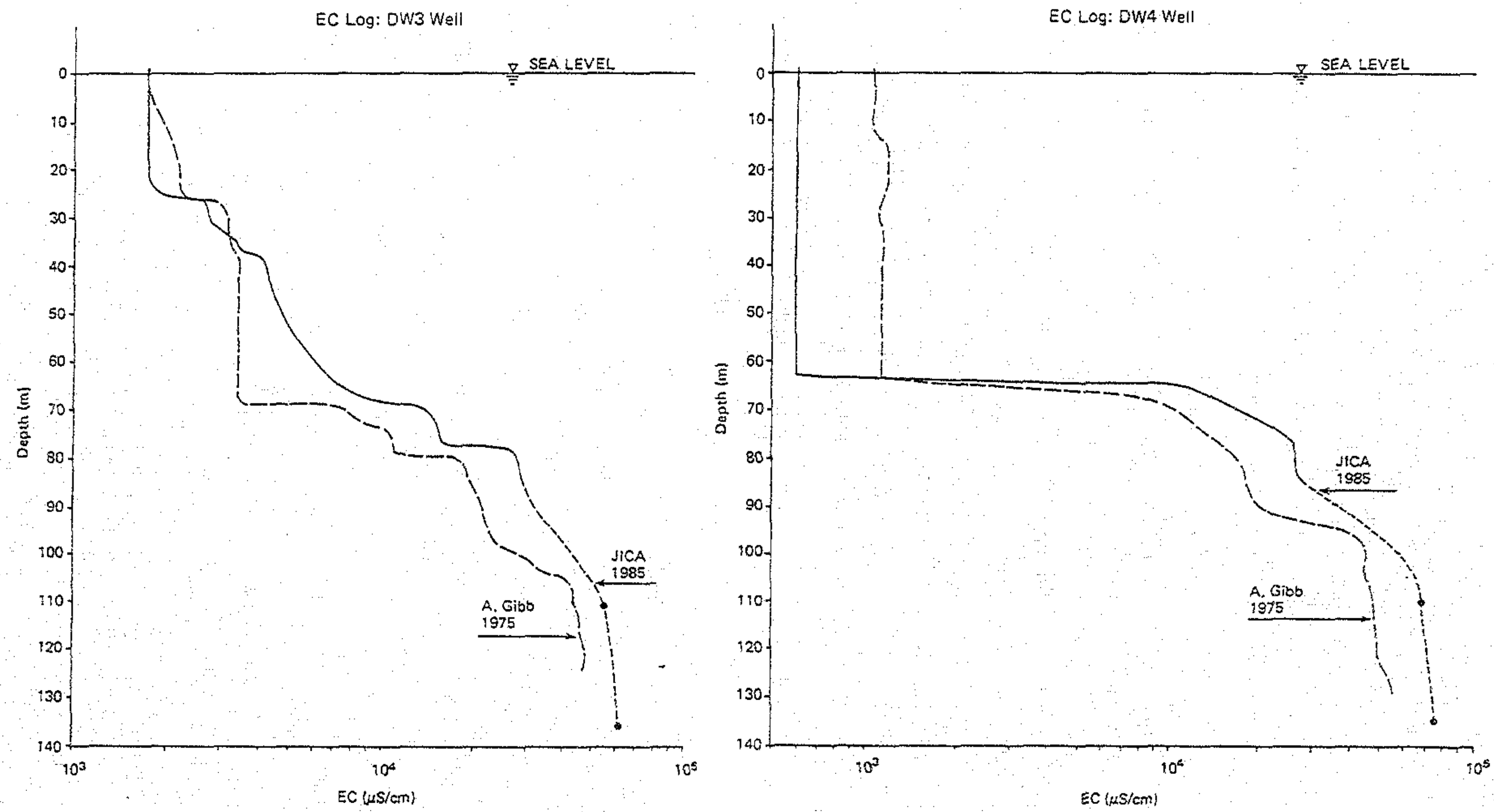

Fig. 4-3-12 (1) EC Log Drift in BA1

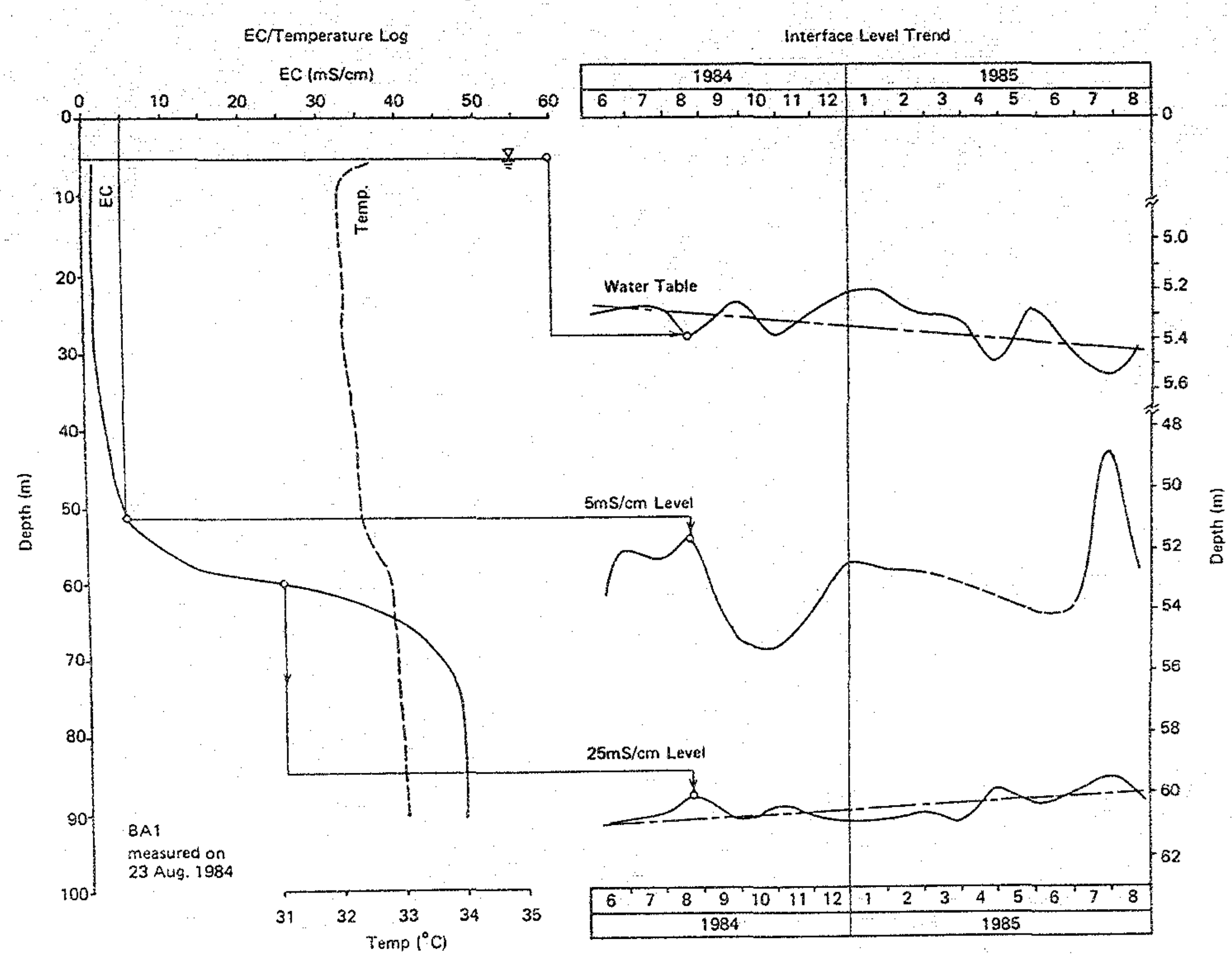

Fig. 4-3-12 (2) EC Log Drift in BF1

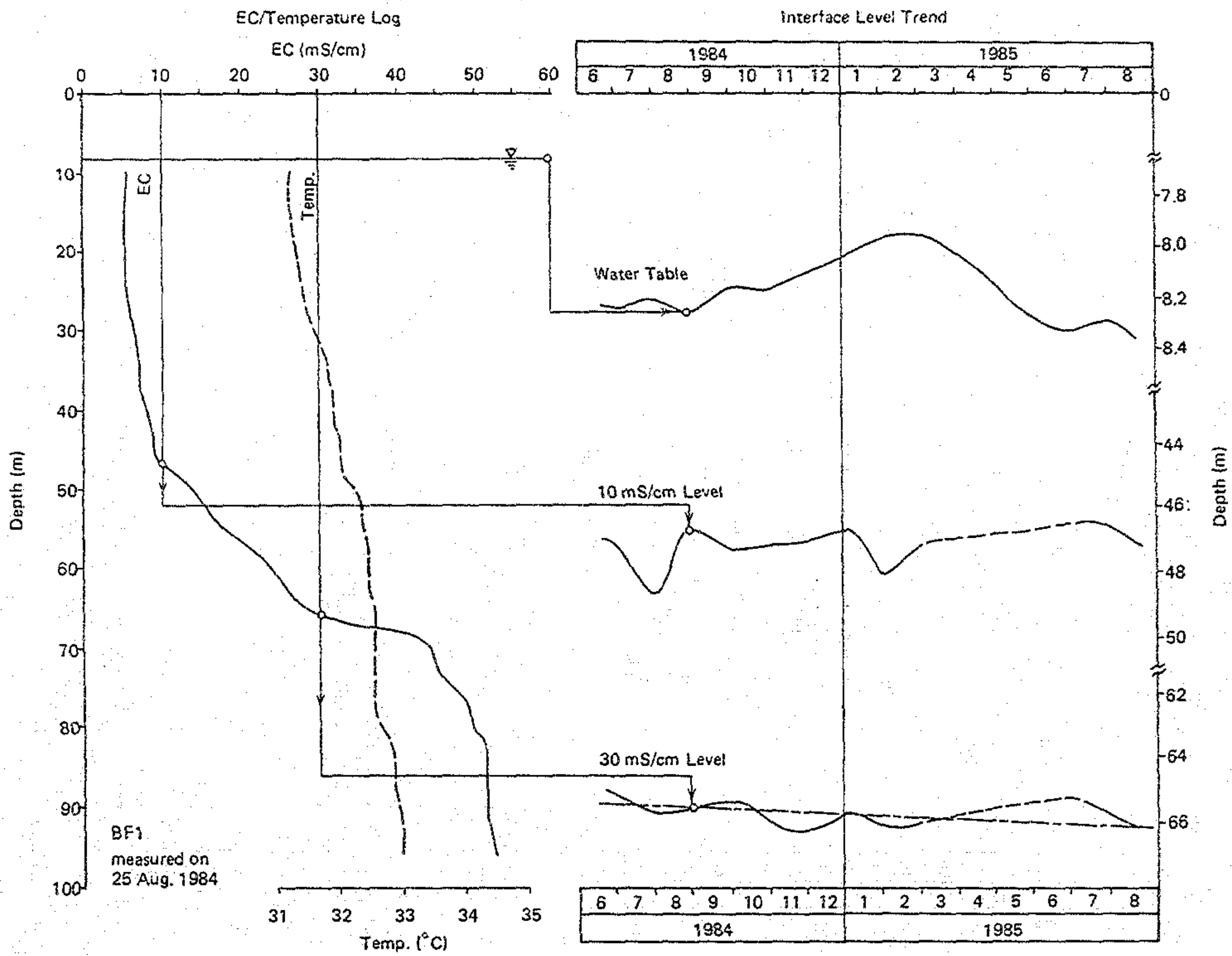

Fig. 4-3-12 (3) EC Log Drift in BM1

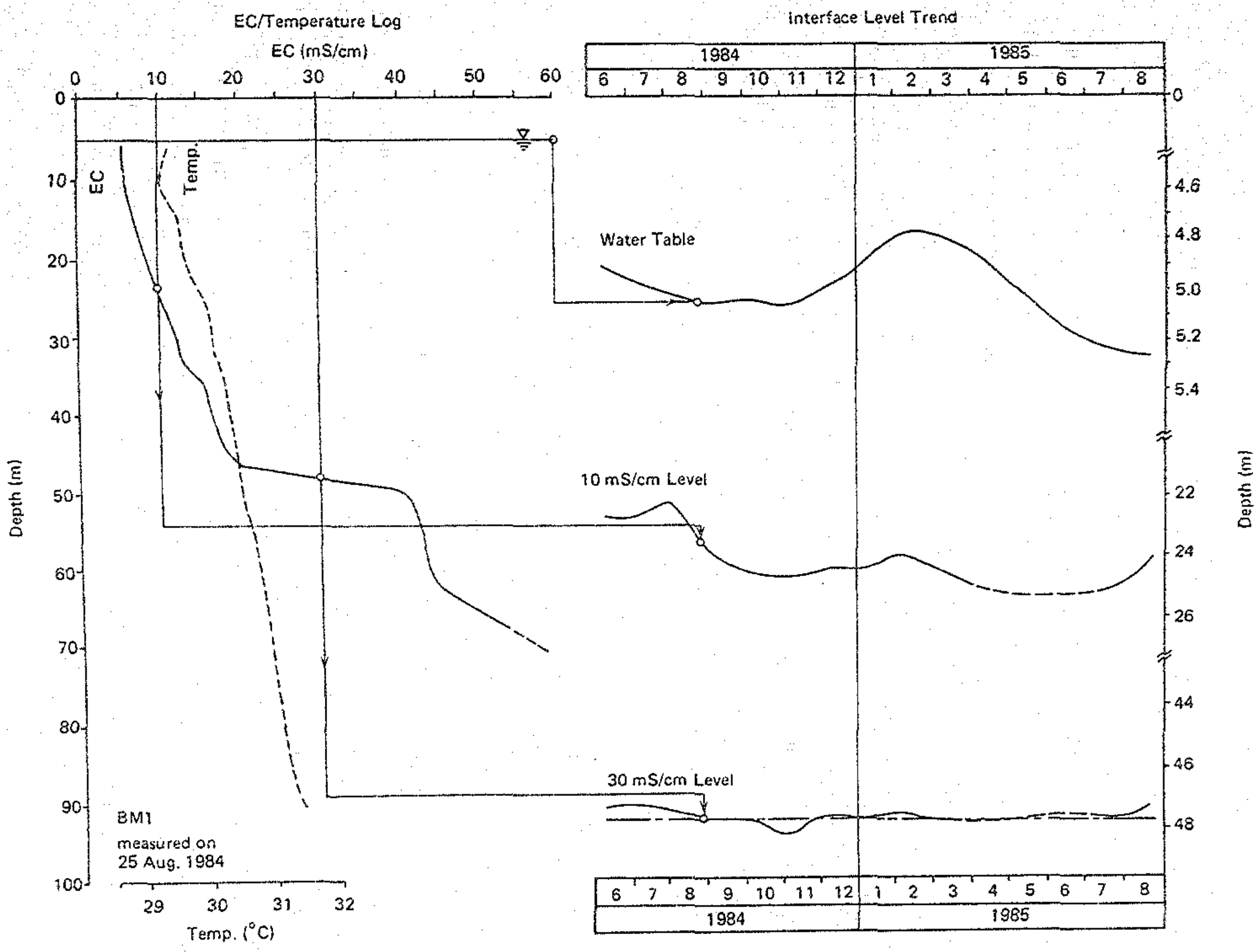

4.4 Groundwater

4.4.1 General Features

Groundwaters in the Project area are classified into six groups: (1) small scale groundwater in the limestone of mountain ridges which issue small mountain springs near the contact between limestone and underlying basement rocks, (2) relatively large-scale groundwater in the massive limestone near the limestone/ ophiolite boundary which issue large hot springs, (3) shallow groundwater in the wadi deposits in the mountains, (4) small-scale groundwater in the ophiolite, where springs are rare, (5) deep-born groundwater in the mid-coastal plain, and (6) shallow groundwater in the coastal alluvium.

Several analytical studies have been applied to these groundwater groups. The study items are as follows:

1. Groundwater temperature
2. Electric conductivity (EC)
3. pH
4. Ionic composition
5. Deuterium and Oxygen-18 content
6. Tritium content
7. Gas composion of hot spring gases

Some data are compiled in Supporting Report D.

As a noteworthy result, analysed data have depicted a groundwater system which is consistent with the geographical distribution of the infiltration property of the ground surface, discussed in Supporting Report B. In this system, due to the poor infiltration in Marginal Wadi Plain which occupies a significant portion of the coastal plain at the up-stream, most of the wadi flood waters do not recharge the groundwater when they run down the wadi bed to the coast. There are two possible recharge zones which are separated by the poor infiltration zone mentioned above.

The upper recharge zone cannot be definitely determined at the present survey level, although the Hajar limestone zone and/or the foothill Tertiary limestone belt fringing the ophiolitic Frontal Mountains are the most probable sites. The lower recharge zone is inferred to be in the belt where Sand/Gravel Plain changes facies from coarse deposit to fine alluvial deposit.

In the following sections, major aspects of analytical results are presented, and in some cases presumable groundwater system is discussed, focussing on the subsurface flow structure and the origin of water.

4.4.2 Groundwater Temperature

During the 1983 survey, considerable number of established observation wells and private production wells were measured of their water temperature when water samples were collected from the water table.

Fig. 4-4-2 shows thermo-contour distribution which depicts a unique bi-maxima pattern. The maxima approximately overlap the deepest water table zones in Fig. 4-4-1.

However, later on, another interesting aspect of the thermal condition was found.

Fig. 4-4-3 was drawn initially with the intention to calculate the regional geothermal lapse rate, using the depth to the water table and the temperatures of the water sample recovered from the depth.

The observed points were classified into three groups: (1) the coastal wells located along the Seeb-Sohar Highway, (2) the midplain wells drilled between the thermal maxima and the highway, and (3) the upper plain wells located at the outskirts of the foothills but up-slope of the mid-plain wells.

The figure has presented a clear-cut distribution of thermal characteristics, where the coastal wells have comparatively wide temperature range with a steep thermal lapse rate (approx. 40°C per 100 m), but the mid and upper plain wells have narrow range and seem to have a homogeneous thermal condition.

The figure does not represent the proper vertical distribution of ground temperature due to the different locations of each well. So the steep thermal gradient should not be regarded as an actual geothermal lapse rate. Instead it may be governed by the groundwater flow, which transport water and heat to the coast, and can be understood better in terms of distance from the coast.

However, the sudden change in the thermal tendency at the mid-plain wells may have resulted from the regional up-welling of deep-born groundwater of homogeneous temperature.

Further investigation is required to confirm the presumed aquifer structure presented above.

4.4.3 Electric Conductivity (EC)

Large number of water samples were measured both of temperature and electric conductivity (EC) at the site.

Fig. 4-4-4 shows the contours of EC in the coastal plain.

EC values reflect the ionic concentration and eventually the salinity of water.

The figure presents a remarkable tendency in which EC does not simply increase toward the coast. Instead, the minimum values are found in the mid-plain.

This is another noteworthy aspect in addition to the thermal aspect discussed in the preceding section.

In conclusion the mid-plain may bear a hydrogeologic structure which still has not been probed into detail. The structure may be responsible for the depressed water tables, the geothermal anomalies and the zones of low EC.

4.4.4 Ionic Composition of Groundwater

Approximately 200 water samples have been analyzed at the Agricultural Research Station of the Ministry in Rumais. Analyzed items were Electric Conductivity (EC), pH, four cations (Na^+, K^+, Ca^{++}, Mg^{++}) and four anions (HCO_3^-, $CO_3^=$, Cl^-, $SO_4^=$). The analyzed data are compiled in Supporting

Report D. Ionic concentrations are presented in milli-equivalent per litre.

By the application of diagrammatic analysis such as Piper's key diagram, we found a chemical trend in the water quality which can be regarded as a general chemical modification of natural water in the Batinah Coast.

Figs. 4-4-5-(1) and 4-4-5-(2) give the result. Fig. 4-4-5-(1) is actual plottings and Fig. 4-4-5-(2) is the explanatory figure. Both diagrams are of Piper's key diagram.

In the diagrams, the water samples are categorized into three groups, bearing a model in which rain causes flood, then flood replenishes shallow aquifer in wadi bed, and the deeper aquifer in the coastal plain is recharged by the shallow aquifer along the wadi course. Consequently, three groups are flood water, non-flood wadi stream water and coastal groundwater.

Flood waters were collected during the wet years in the beginning of this project at several wadis, mostly at the later part of recession stage. Wadi stream waters were collected, being regarded as representing the shallow wadi bed aquifer. Coastal groundwaters were collected from various locations; however, sampling frequency was less inland due to the present distribution density of the observation wells. Instead a great number of wells were available in the coastal agricultural belt.

Fig. 4-4-5-(2) is referred to in the following discussion. As expected prior to the analysis, flood waters have been found in proximity with rain water of their ionic composition, i.e. their alkali earth metal ions and bicarbonate and carbonate ions prevail over alkali metal and chloride and sulfate ions. The flood water occupies in a relatively narrow area in the diagram. It is well known fact that rain water contains more alkali earth metal and bicarbonate/carbonate ions because of its passage through the atmosphere. So the flood in the Batinah can be regarded as a product of the direct surface runoff from rain. This flood process is not usual in temperate climates in which floods are the discharge from the increased groundwater caused by the quick infiltration through the densely vegetated ground surface. Stable isotope analysis also confirmed the origin of the floodwater in the Batinah as direct runoff from rain.

Wadi waters have been identified just at the transitional part between flood water and coastal groundwater in the diagram. This is also reasonable in terms of our groundwater replenishment model.

However, coastal groundwater covers a wide range of ionic compositions as shown in the diagram, although it shifts to the points in the diagram much more enriched in alkali metal ions and chloride ions. This is again agreeable, for the alluvial deposits in the coastal plain contain more clay minerals and clay minerals may undertake ionic exchange in preference to alkali metal ion. Chloride ion is just simply enriched as a most stable anion in the solution.

In conclusion, we may describe the modification of the Batinah groundwater as follows:

Rain replenishes the shallow groundwater as carbonate hardness type, the shallow groundwater shifts into the intermediate type, and then most groundwater converges into non-carbonate hardness type. Non-carbonate hardness type water is generally typical in spring and fossil waters.

Coastal groundwater has a wide diversity of chemical properties, reflecting the diversity in the mineral composition of the alluvial deposit there. More detailed classification could be done later.

4.4.5 Stable Isotope Content of the Batinah Water

During the Project, about 330 water samples have been collected for stable isotope analysis. We have selected 150 samples to be analyzed of O-18 (Oxygen-18) and D (Deuterium). The analyzed data, compiled according to the sample origin, are printed in Supporting Report D.

The analyzed data are presented as permill deviation values, δO-18 or δD, based on standard reference water, namely SMOW (Standard Mean Ocean Water) available from IAEA (International Atomic Energy Agency), Vienna, Austria.

δX : X is either O-18 or D, is formulated as follows:

$$\delta X = \frac{R(X) - R(X)_0}{R(X)_0} \times 1{,}000$$

Where $R(X)$ and $R(X)_0$ are absolute isotopic ratios of the sample and the reference, respectively. The absolute isotopic ratios of R(O-18) and R(D) in the SMOW are about $2{,}000 \times 10^{-6}$ and 150×10^{-6}, respectively.

Fig. 4-4-6 is the diagram of all the data presented. This may represent the range of stable isotope content in the natural water in the Batinah. δO-18 distribution occupies between -8‰ and +8‰, and δD between -45‰ and +45‰.

Some of the rain waters are remarkably enriched with the heavier isotope: typical in the arid region. Measured values are widely distributed in the diagram and indicate that precipitation takes place in a great environmental diversity.

Instead groundwater occupies relatively narrow space in the diagram. This suggests that replenishment occurs in a rather restricted way.

Flood waters are found outside the zone of groundwater and overlap the rain water. This clearly indicates that the floods are directly discharged from the rain quite frequently in the Batinah.

As the analytical results derived from the ionic composition in combination with the stable isotope contents, Fig. 4-4-7 is presented for the coastal groundwater.

In this figure ionic ratios between alkali earth metal and alkali metal are plotted against δD. Each plot is also indicated with different symbols according to its electric conductivity (EC).

The ionic ratio seems to increase when δD decreases, but the correlation could be poor.

However, once we examine the diagram, considering the EC values, there we find clear tendency in which higher EC water are distributed in a narrower zone of diagram than the lower EC waters.

The ionic ratio is regarded as an indicator which reflects age and subground passage of groundwater, especially likely to the groundwater in alluvial deposits as stated in the previous section. If we focus the matter in terms of the age of groundwater, the ionic ratio decreases as time passes due to the increase of the alkali metal ions.

The groundwater is initially replenished by rainwater, and rainwater has wider range in δD, higher ionic ratio and lower EC. So the fresh and shallow groundwater could have such property and this may form the widest distribution in the diagram.

In the diagram, the distribution is apt to converge into a certain narrow range of δD as EC values increase. Except for two data near $\delta D = 0‰$, the plotted data seem to form a zone around $\delta D = -7‰$. This suggests that the aged groundwater of high EC and low ionic ratio has relatively homogeneous δD level. δD of $-7‰$ is relatively depleted value in the Batinah, so we presume the deep-born aged groundwater may have its origin in a certain inland zone. In many localities in the world, δD of rain has been observed to decrease inland. The phenomenon is explainable by the isotope fractionation process in which the precipitation mechanism in a closed air mass leaves the heavier isotope component in the precipitate.

A similar presumption is to be presented in the discussion on tritium contents.

4.4.6 Tritium Content of the Batinah Water

In the previous water resources projects some analyses of tritium of the natural waters in Oman were carried out. Among them Gibb (1976) reported the most surprising data. They presented a figure in which the coastal groundwater appeared at zero level of tritium. The zero level zone extended inland considerably, so in the coastal plain there seemed to exist no recently replenished groundwaters. The initial tritium survey was of preliminary level, so it was required to conduct some more detailed studies on the coastal groundwaters.

Sixty water samples of various origins were collected in the 1982/1983 period of this project with a special preference of the coastal shallow groundwater. The sampled wells of shallow groundwater were located along the Seeb-Sohar highway and selected by geographical consideration in order to clarify the local drainage effects.

Tritium is a radio-active hydrogen isotope naturally produced by cosmic rays. But the thermo-nuclear experiments in the atmosphere in 1950s and 1960s dramatically increased the artificial tritium level in the natural environment.

Tritium has a half-life of 12 years. The natural tritium level in water has been measured to be around 1 T.U.: which is equal to 10^{-18} in the tritium vs. hydrogen ratio.

Any natural water of less than 1 T.U. is regarded as aged water originated from the rain prior to 1950s.

Fig. 4-4-8 shows the distribution of analized T.U. Level. The analyzed data and the location of the samples in classified sample groups are listed in Supporting Report D.

The figure shows three zones of tritium level distribution running along the coast line: (1) The zone of the highest level in major mountain and foothill region, (2) the zero level zone in midplain, and (3) admixtured level zone in coastal strip. This zonal distribution is presumed to reflect a groundwater replenishment system in which two intensive replenishments, i.e. infiltration zones, are imminent: one in the foothill or inland and the other in the coastal alluvial plain.

In the figure there are some more noteworthy points.

In Wadi Ahin in the west, coastal well waters contrast outstandingly each other in their tritium level. The west bank wells contain more than 5 T.U., but adjacent wells on the east bank is at zero level although they are located nearby, approx. 1 km apart, and are very similar in ionic composition.

In the eastern coastal area , higher tritium contents are not always located near the major wadi beds. Instead they tend to appear at the terminal points of inter-wadi basins. The majority of coastal wells have zero level of tritium content.

These points suggests that there are some groundwater replenishments in the coastal strip but they are neither frequent nor significant. Most of the flood water may just be discharged into the sea or evaporated even when located inland of the coastal farming zone.

Fig. 4-4-9 depicts tritium and deuterium contents of the coastal groundwater. Except for three conspicuous plots, there appears a trend where inferably young groundwaters of low EC and high tritium level have wider δD range. As EC value increases, tritium level becomes lower and δD converges to a narrower range around -7‰. Here again the aged groundwater seems to be replenished somewhere inland with the water of rather homogeneous deuterium content.

4.4.7 Gas Composition of Bubbling Gases of Hot Spring

It is well known fact that there are many hot springs in Oman. In the Project area there are four famous ones. All of them have bubbling in various intensities. Previously Gibb (1976) reported this phenomenon , and their gas analysis was made about the ordinary gas species such as oxygen, nitrogen, hydrogen, carbon dioxide and some hydrocarbons. The most noticed aspect of their results was about the hydrogen gas content. Hydrogen gas was extraordinarily rich in the bubbles of spring water in the Semail ophiolite zone. It sometimes exceeded 80%.

In the present analyses bubbling gases both from the ophiolite zone spring and the Hajar limestone zone springs are analysed.

However, this time we analysed inert gases in addition to the ordinary gases. The results are presented in Table 4-4-1.

As already reported by Gibb (1976), nitrogen gas is predominant in the bubbles of the limestone hot springs. But we detected some inert gases amounting 1 percent or so. Among them almost 1/10 is occupied by helium and it indicates a remarkable enrichment of helium in contrast to the atmosphere. The enrichment can be regarded as caused by the isotopic decay of radioactives in the rocks. Helium-3 and Helium-4 ratio clearly shows an apparent increase of Helium-4 in the hot spring bubble, comparing with the atmosphere. Helium-4 is a famous decay product of uranium, a radioactive, which is always contained in some amount in rocks.

The hot springs are presumably receiving heat from the radioactive decay and only can attain the temperature around 70^{o}c. These trace elements may contribute some important conclusions for tracing and identification of groundwater in the future.

Fig. 4-4-1

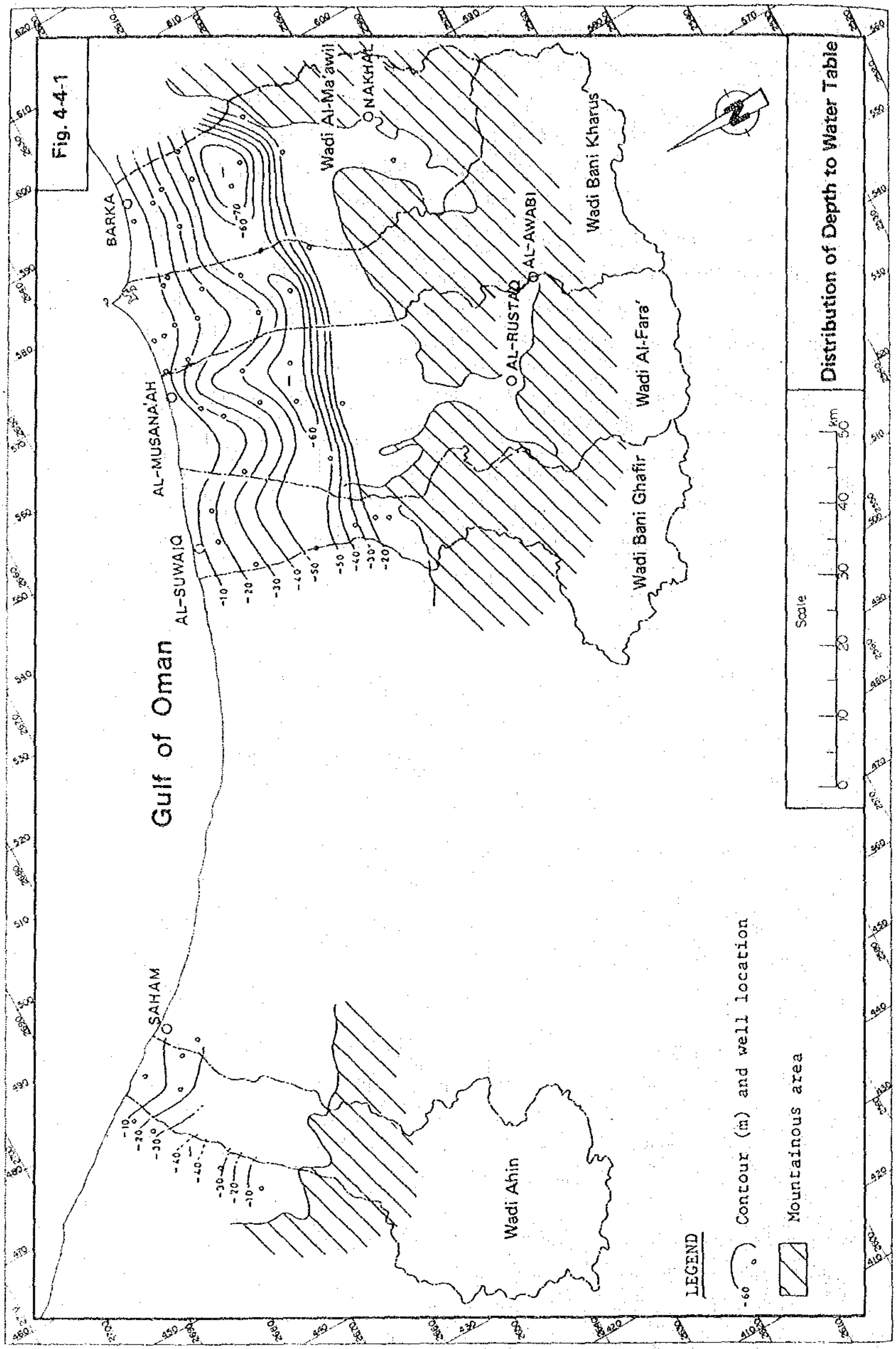

Distribution of Depth to Water Table

Fig. 4-4-2

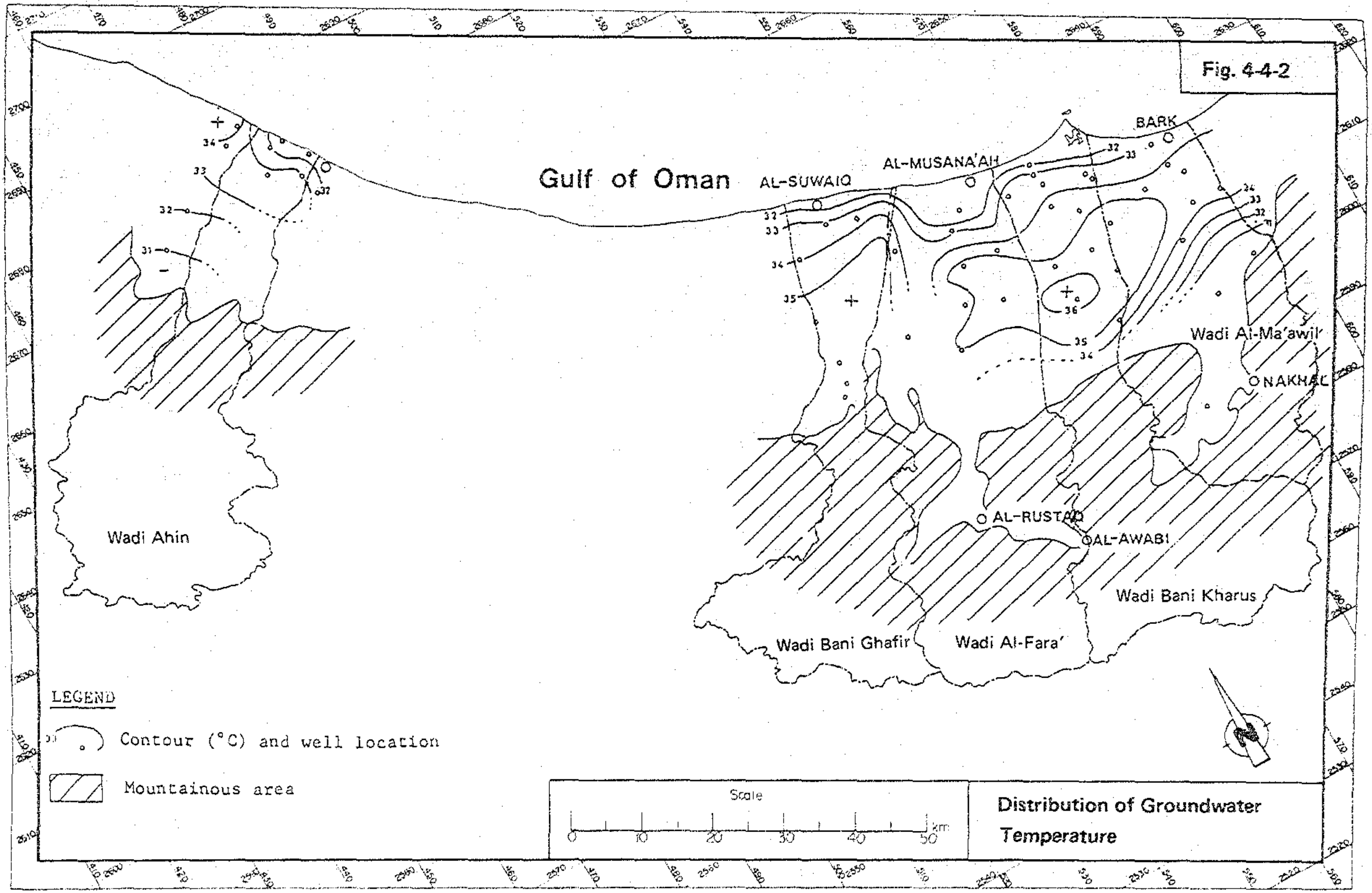

Distribution of Groundwater Temperature

Fig. 4-4-3 Groundwater Temperature vs. Depth to Water Table

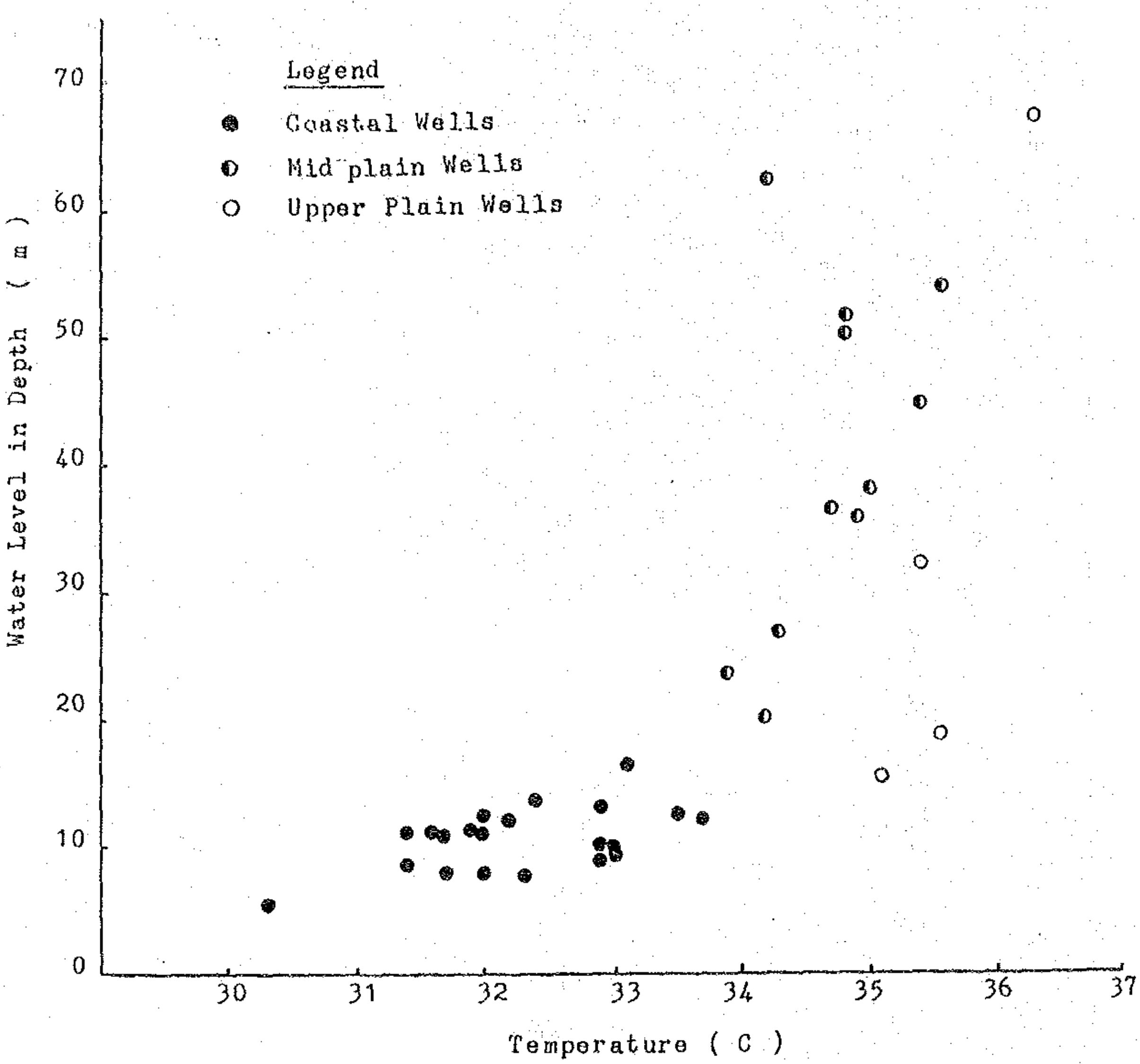

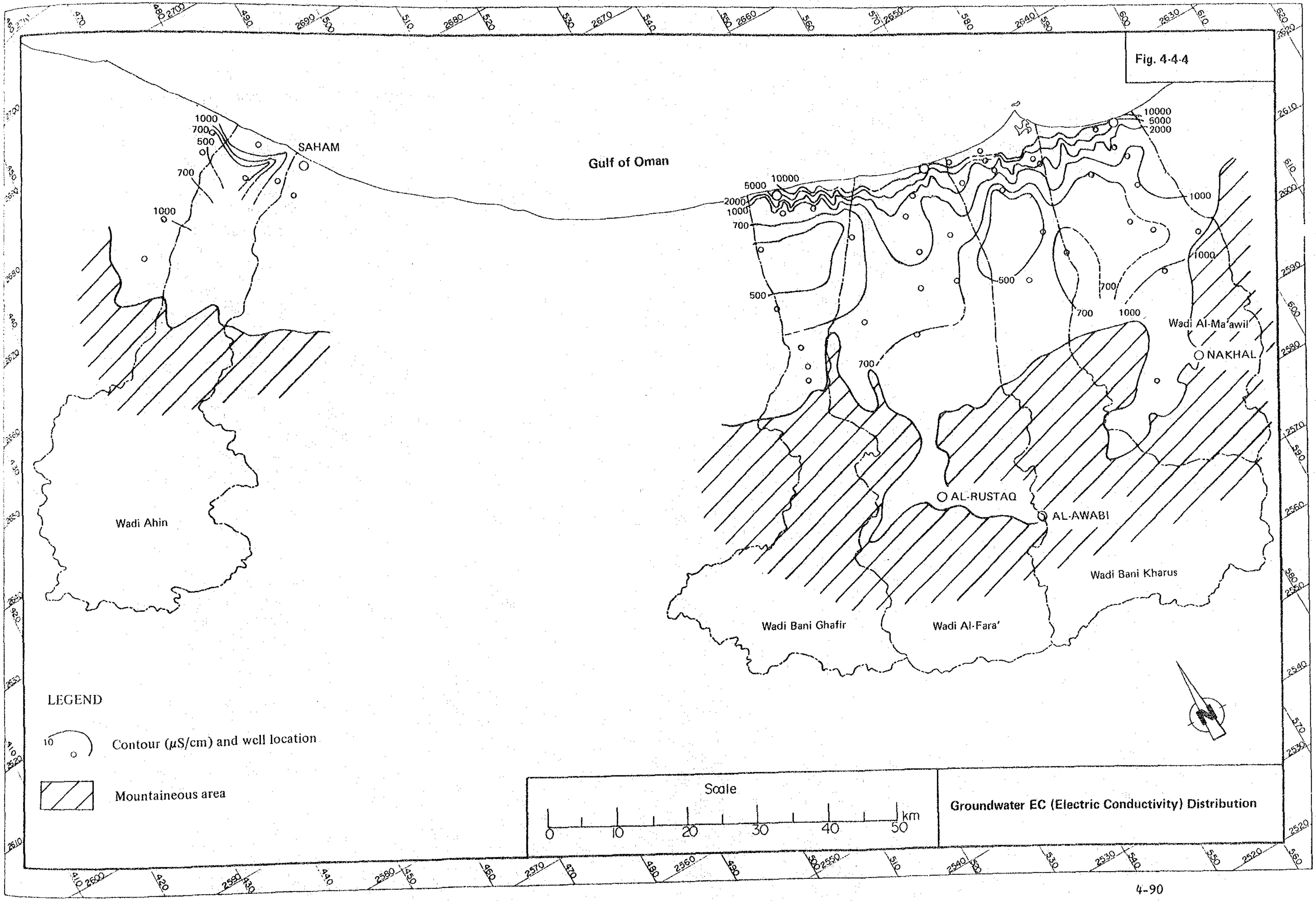

Groundwater EC (Electric Conductivity) Distribution

Fig. 4-4-5(1) Piper's Key Diagram of Batinah Water

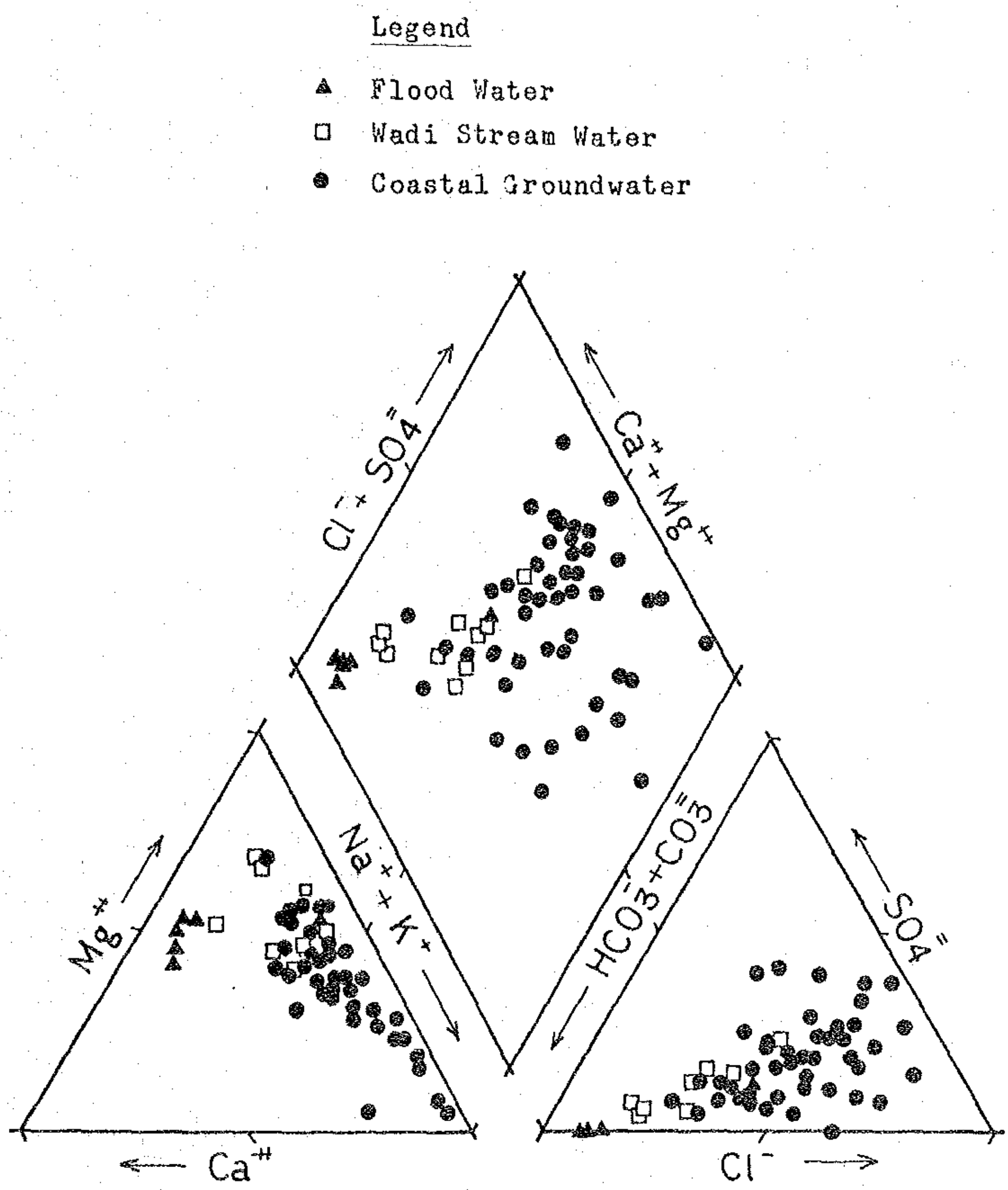

Fig. 4-4-5(2) Schematic Piper's Key Diagram of Batinah Water

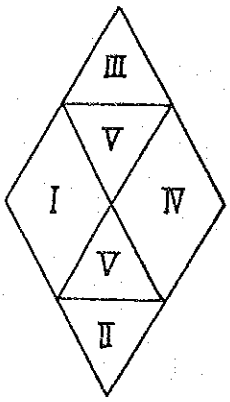

Chemical Classification

I Carbonate Hardness Type
II Carbonate Alkali Type
III Non-carbonate Hardness Type
IV Non-carbonate Alkali Type
V Intermediate Type

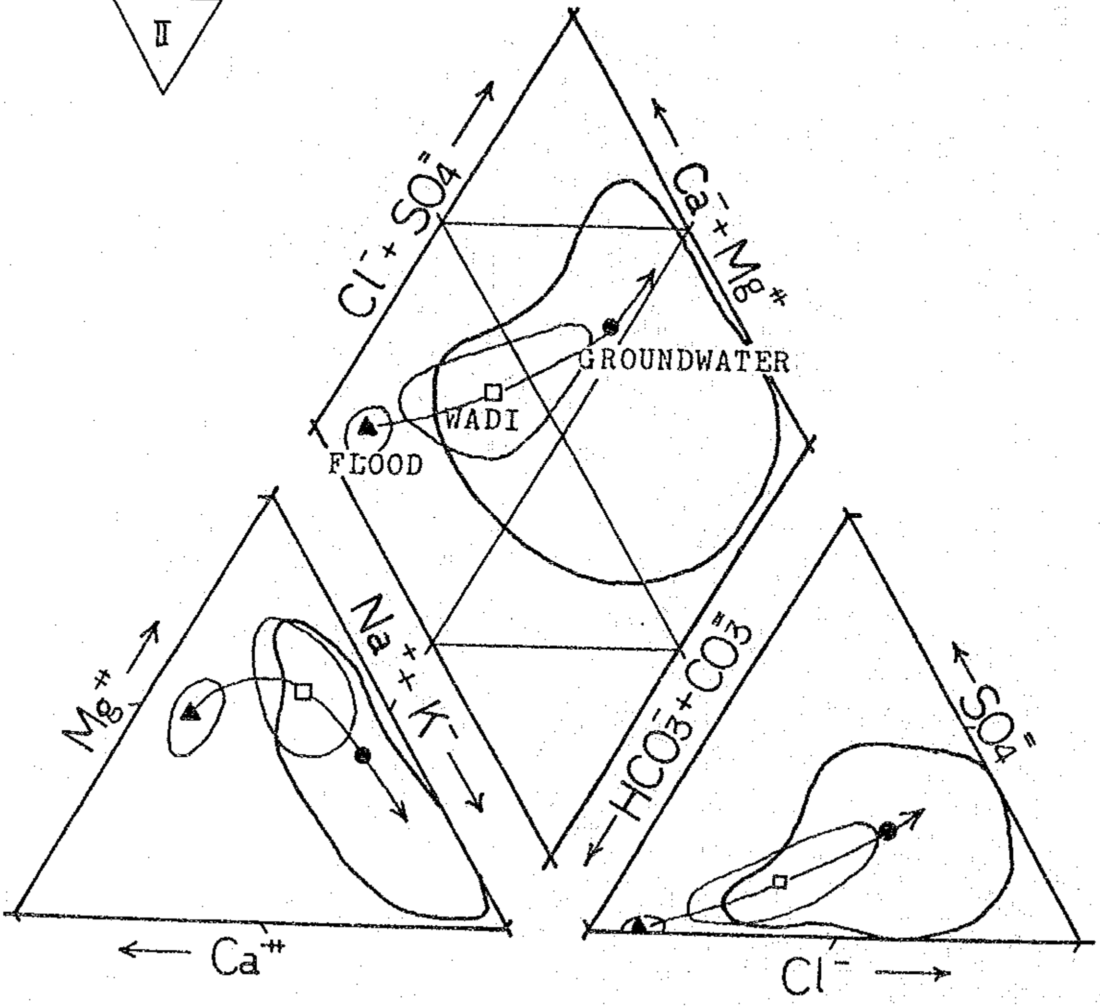

Fig. 4-4-6 δD vs. $\delta^{18}O$ of Natural Water in the Batinah

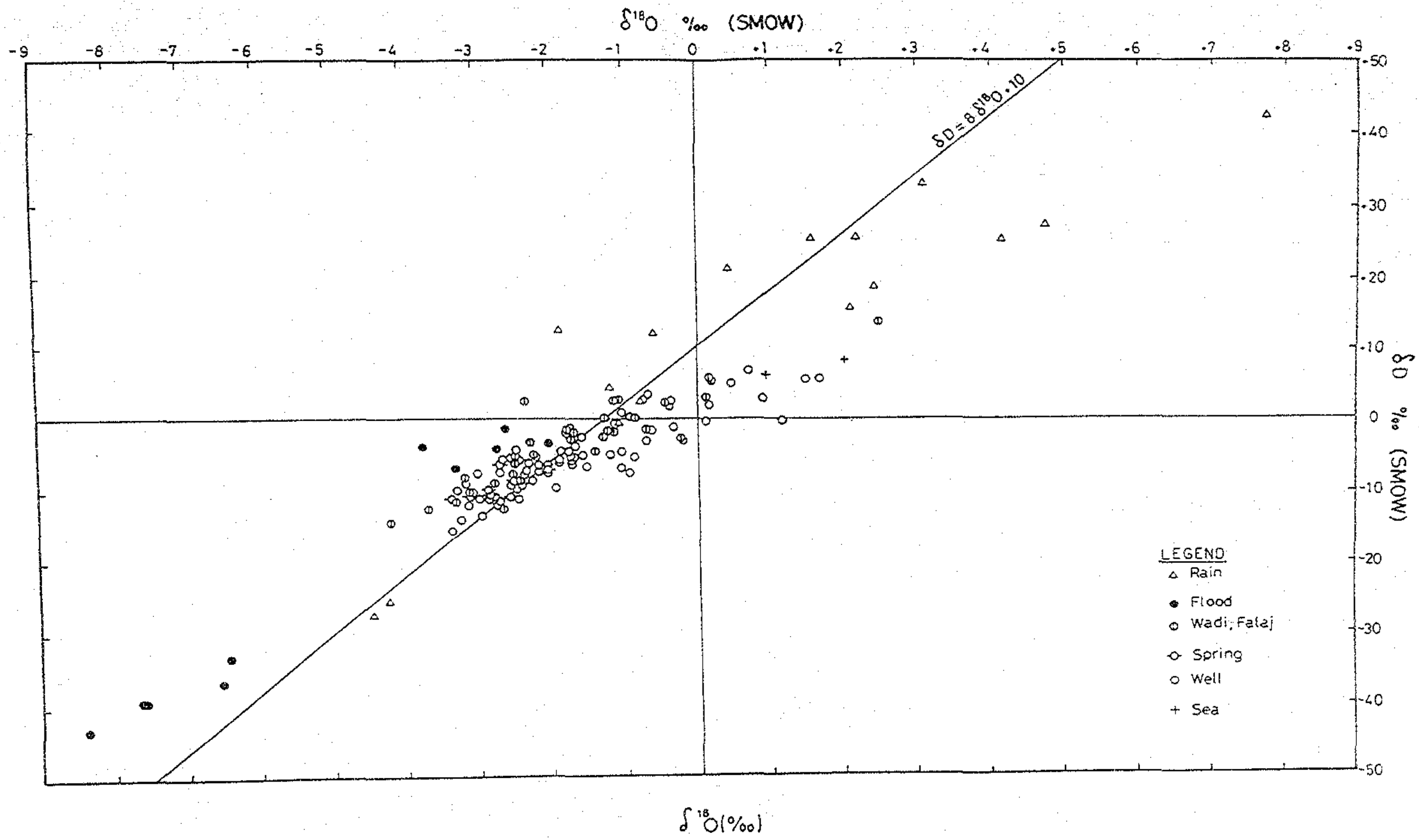

Fig. 4-4-7 $\frac{[Ca^{++}]+[Mg^{++}]}{[NA^{+}]+[K^{+}]}$ vs. δ D of Coastal Groundwater in the Batinah

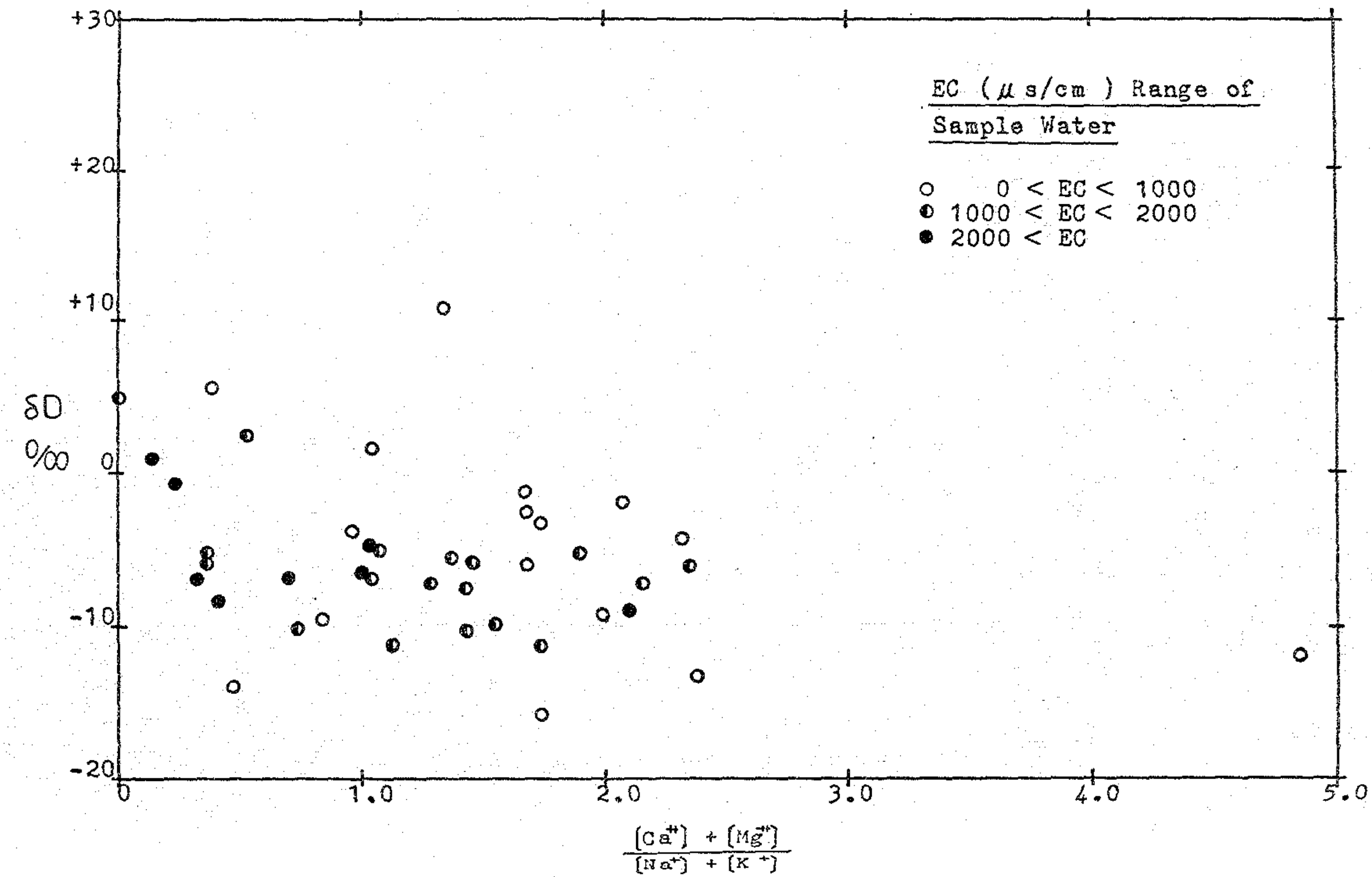

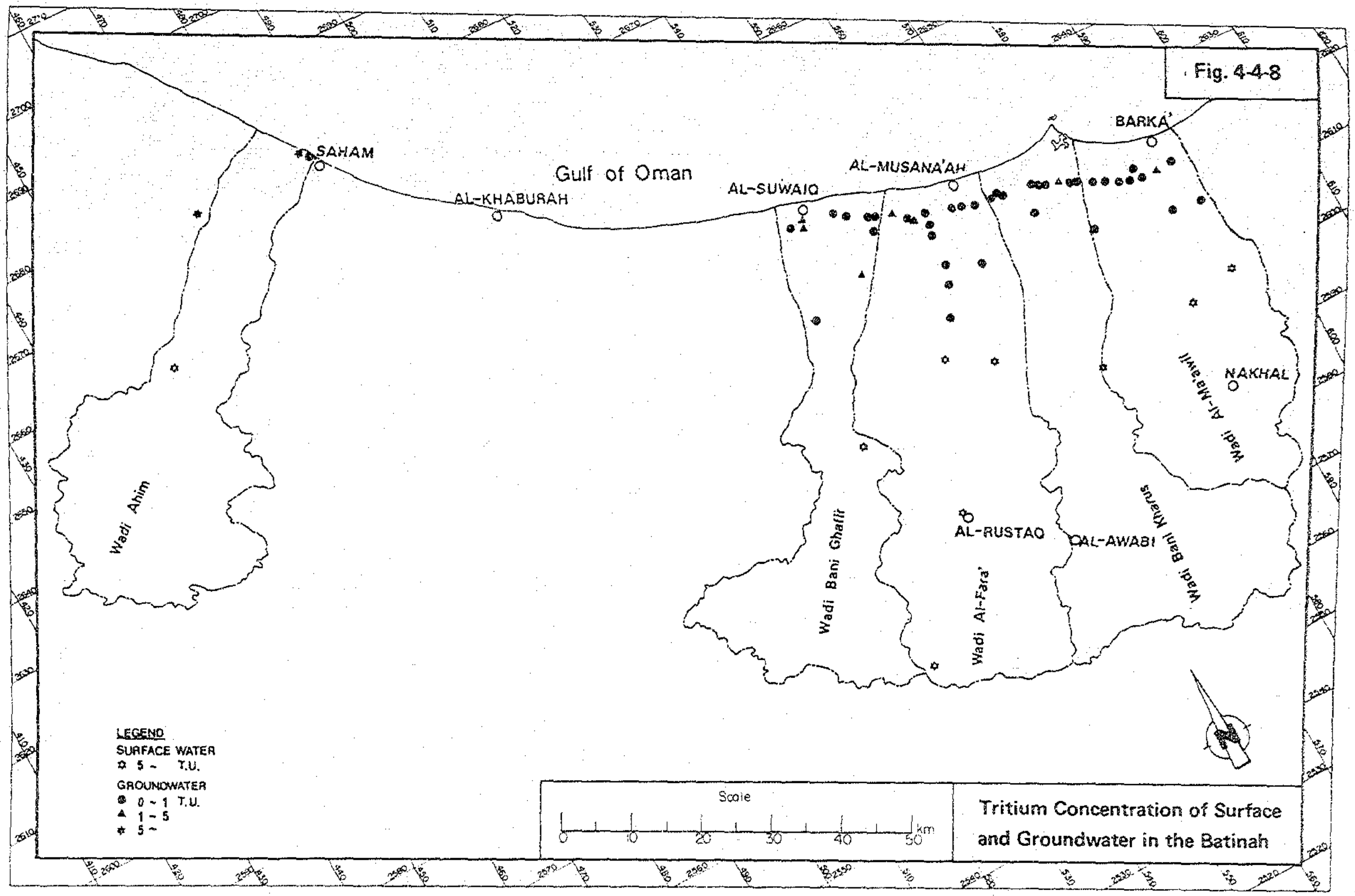

Fig. 4-4-8

Tritium Concentration of Surface and Groundwater in the Batinah

Fig. 4-4-9 Tritium and Deuterium Content of Coastal Groundwater in the Batinah

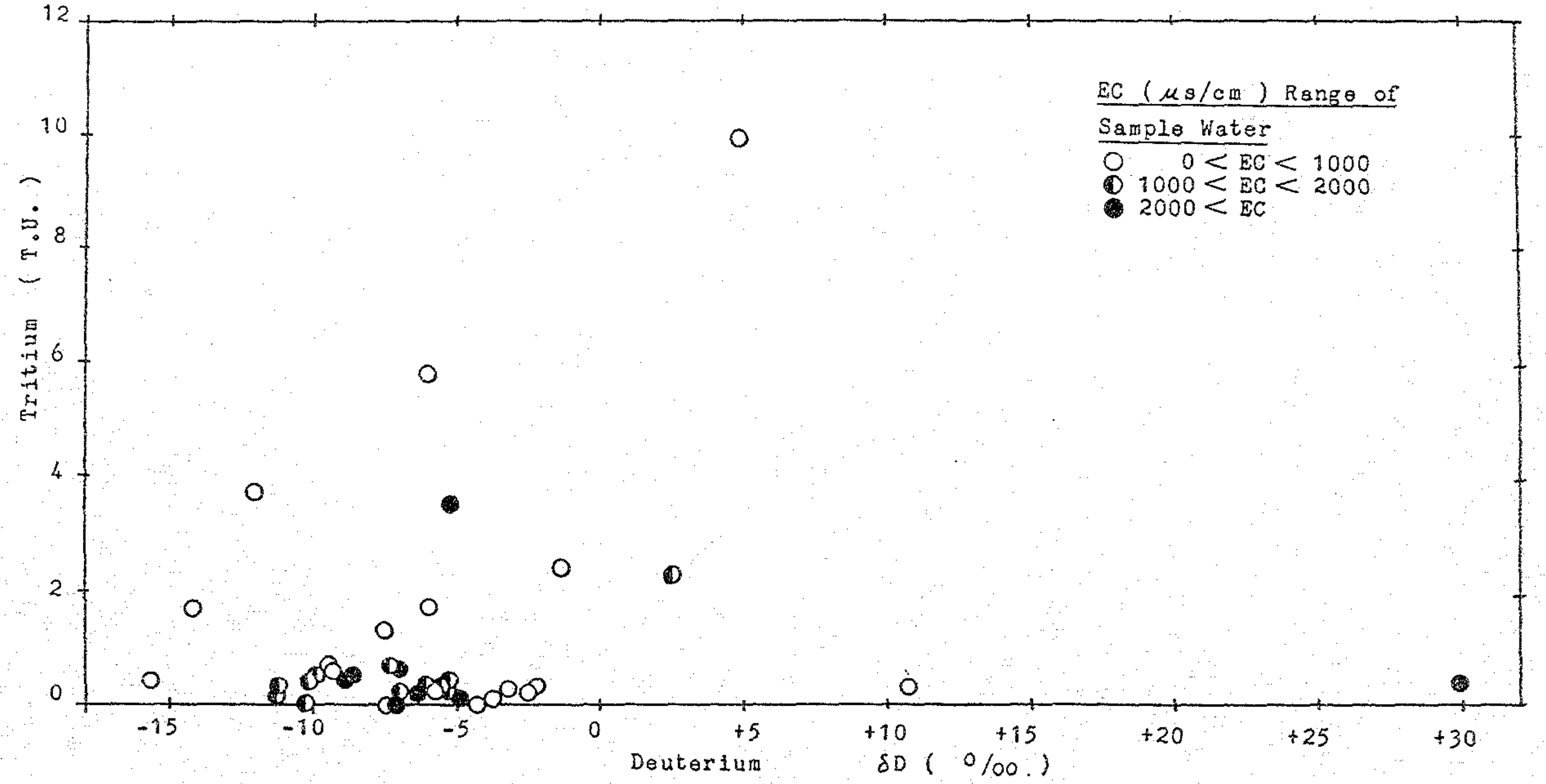

Table 4-4-1 Chemical and Isotopic Compositions of Hot Spring Gases

No.	Location	Associated water Temp. °C	pH	Chemical composition H_2 %	N_2 %	CO_2 %	CH_4 %	O_2 %	Ar ppm	He ppm	Ne ppm
1	Ain Al-Waddah*	32.0	9.5	81.0	15.9	<0.1	2.22	0.54	3290	<5	<5
2	Howqain Hammam	42	9.5	69.0	28.1	<0.01	2.23	0.18	5100	<5	<5
3	Ain Al-Kesfah	45.7	6.5	200ppm	72.9	1.46	<0.002	24.8	7610	930	10.9
4	Ain Al-Shubaikhah	52.1	6.3	<5ppm	91.2	4.80	0.0018	3.0	9390	1240	13.4
5	Hammam Al-Ali	67	6.3	<1ppm	91.8	4.4	0.008	2.5	12100	297	18.1
6	Air			0.5ppm	78.1	0.03	2ppm	20.9	9340	5	18.2

No.	Location	Associated water Temp. °C	pH	Isotopic composition N_2/Ar	δD_{H_2} ‰	$\delta^{13}C_{CO_2}$ ‰	$\delta^{13}C_{CH_4}$ ‰	$\delta^{15}N_{N_2}$ ‰	$^3He/^4He$ $\times 10^{-7}$	$^{40}Ar/^{36}Ar$
1	Ain Al-Waddah*	32.0	9.5	48	-560	–	-34.5	+0.9	5.89	300
2	Howqain Hammam	42	9.5	55		–			10.0	295
3	Ain Al-Kesfah	45.7	6.5	96	–		–		1.32	300
4	Ain Al-Shubaikhah	52.1	6.3	97	–	-10.7	–	-0.5	1.76	303
5	Hammam Al-Ali	67	6.3	76	–	-9.6	–	0.0	5.30	296
6	Air			84		-8	-47	0.0	14.0	295.5

Contents of H_2S are less than 0.01%.
Ratios δD, $\delta^{13}C$ and $\delta^{15}N$ are relative to SMOW, PDB and atmospheric nitrogen, respectively.
*Oman Interior